ISSN 2039-7941
Anno 2017_Numero 380

rapporti tecnici INGV

The 2016 field campaign of La Solfatara volcano: monitoring methods and instruments for volcanic surveillance

380

Istituto Nazionale di Geofisica e Vulcanologia

Segreteria di Redazione
Francesca Di Stefano - Referente
Rossella Celi
Tel. +39 06 51860068
redazionecen@ingv.it

in collaborazione con:
Barbara Angioni (RM1)

REGISTRAZIONE AL TRIBUNALE DI ROMA N.173 | 2014, 23 LUGLIO

Rappresentante legale: Carlo DOGLIONI
Sede: Via di Vigna Murata, 605 | Roma

ISSN 2039-7941
Anno 2017_Numero 380

rapporti tecnici INGV

THE 2016 FIELD CAMPAIGN OF LA SOLFATARA VOLCANO: MONITORING METHODS AND INSTRUMENTS FOR VOLCANIC SURVEILLANCE

Malvina Silvestri[1], Jorge Andres Diaz[2], Enrica Marotta[3], Giorgio Dalla Via[3], Eliana Bellucci Sessa[3], Teresa Caputo[3], Maria Fabrizia Buongiorno[1], Fabio Sansivero[3], Massimo Musacchio[1], Pasquale Belviso[3], Antonio Carandente[3], Rosario Peluso[3], Rosella Nave[3], Giuseppe Vilardo[3], Fawzi Doumaz[1], Ernesto Corrales[2]

[1]**INGV** (Istituto Nazionale di Geofisica e Vulcanologia, Centro Nazionale Terremoti)
[2]**GASLAB, CICANUM** (Universidad de Costa Rica, San Josè, Costa Rica)
[3]**INGV** (Istituto Nazionale di Geofisica e Vulcanologia, Sezione di Napoli - Osservatorio Vesuviano)

380

How to cite: Silvestri M. et al., (2017). The 2016 field campaign of La Solfatara volcano: monitoring methods and instruments for volcanic surveillance. Rapp. Tec. INGV, 380: 1-42.

Index

1. Fieldwork Overview

For the purpose of testing miniaturized instruments for volcanic monitoring, a field campaign on La Solfatara volcano was planned and carried out from 21 to 24 September 2016. The results obtained from the previous field campaigns performed in this same volcano in 2014 and 2015 [Silvestri et al., 2015 and 2016] are being used for comparison to determine the improvements required on the miniaturized instruments as part of an ongoing collaboration within the different institutions. The research was done in close cooperation among INGV, the University of Costa Rica and the U. S. Geological Survey. The La Solfatara volcano is a tuff cone located in the central part of the repeatedly collapsed Campi Flegrei caldera (in the south of Italy), which is continuously monitored by INGV through permanent network and field campaigns. Volcanic activity is expressed through fumarole emissions that are most active within the crater, thermal pools, and regions with seismic activity. The entire area is characterized by a diffuse degassing [Chiodini et al., 2001] even if the fumarolic activity is mainly concentrated in its south-eastern part. In this report, the measurements collected with different instruments such as MiniGAS, Mini Mass Spectrometer mounted on a drone, thermal camera, spectro-radiometer and measurements with satellite data are reported.

2. Instruments

2.1 MiniGAS NTX

The MiniGAS is a multisensor instrument in development by Dr. Diaz since 2010 and targeted for unmanned airborne deployments to characterize volcanic gas emissions. Alpha and Beta versions of the MiniGAS payload have been flight tested within the Turrialba volcano plume onboard the Vector Wing 100 UAV [Pieri et al., 2013] and on tethered balloon airborne platforms, generating real time 3D gas concentration plots of the active volcanic plume. It includes sensors for atmospheric parameters such as temperature, pressure and relative humidity like any radiosonde, but also includes gas sensors to measure the concentration of gases such as SO_2, H_2S and CO_2 combined with GPS to geolocate all the measured parameters. The data is stored onboard an SD card and also sent by telemetry via radio for real time data display and in the event that if the aircraft is lost, the data is saved on the mission control center computer, (Figure 1).

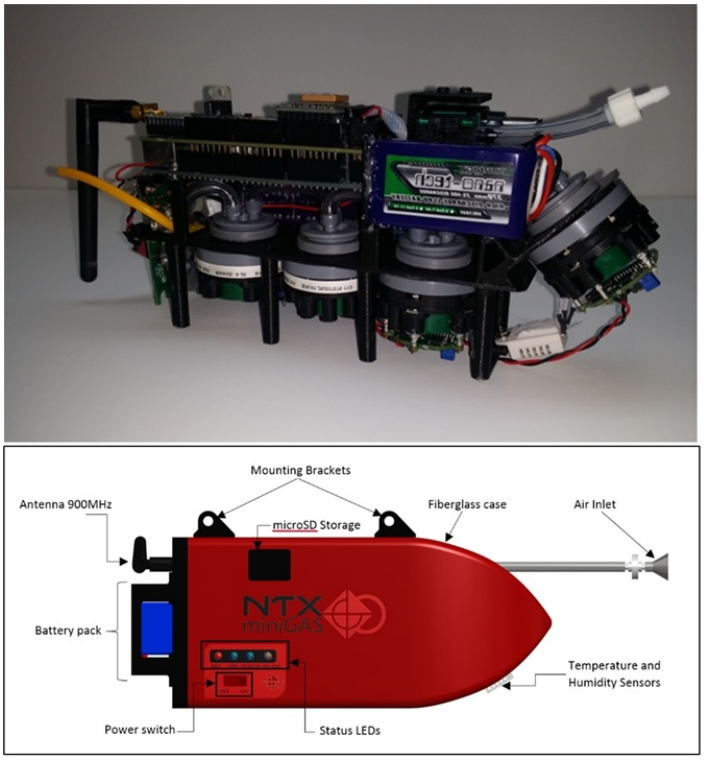

Figure 1. Internal and external structure of the MiniGAS multi sensor instrument.

In 2014, the Alpha version of the MiniGAS was deployed at La Solfatara volcano to characterize the fumarolic activity conducting surveys either by hand carrying the instrument into the fumaroles ("sampling walk") or flying by drone on board a Phantom 1 DJI Quadcopter [Silvestri et al., 2015]. Then in 2015 both Alpha and Beta versions of the MiniGAS were deployed at La Solfatara and Vulcano Island on board a DJI S800+ and Italdrone Octocopters [Silvestri et al., 2016].

The NTX version of the MiniGAS (Figures 1 and 2) was deployed at La Solfatara volcano in the 2016 mission and used an improved Arduino mainboard that connects all the different components: 200ppm electrochemical sensors (CityCel) for SO_2 and H_2S detection, and an improved 5000ppm non-dispersing near infrared for CO_2 detection (NG Gascard from Edinburg Instruments). *In situ* sampling was achieved by injecting an airstream into the multisensor with a very small displacement pump (1.2 lpm) and having all sensors connected in cascade after the pump to maintain head pressure more constant on sensor face. It is also possible to add two additional sensors to the payload (such as H_2 and CH_4 for other applications, see Badalamenti et al, 2001, Roberts et al, 2012 and 2014). The NTX MiniGAS version had a total weight of 1.2 kg including a 2200mAh battery providing 6 hrs of continuous operation. The data collection was improved to from 0.3 to 1 Hz scan rate and onboard data storage was accomplished via 16GB micro-SD card and telemetry via Xbee Pro 900MHz antennas to provide 1 km range. Finally, a waterproof aerodynamic fiberglass cover was designed to protect electronics from the harsh environment, lowering the drag in the air and painted metallic red to easily spot the payload in the case for a crash.

The main characteristics of MiniGAS NTX can be summarized in the following table:

Characteristic	**Parameter**
Dimensions	11" x 5" x 4.5" (L x H x W)
Weight	1.2 Kg (with battery)
Battery	12VDC, Lithium Polymer
Operating time	6 hours (with 1600mAh Batt.)
Sampling Rate	1 Hz (configurable)
Capacity data Storage	16 GB
Telemetry Range	2 Km (tested)
Nominal Frequency	900 MHz
Case	Fiberglass

Sensor	**Model**	**Range**	**Accuracy**	**Resolution**
Pressure	BMP180	300 to 1000 hPa	± 0.12 hPa	0.01 hPa
Temperature	DS18B20	-55°C to 125°C	± 0.5°C	9 to 12 bits
Humidity	SHT10	0 to 95%	± 4.5%	0.4% RH
SO_2	Cititech EZT3ST/F	0-200 ppm	1% FS	0.5 ppm Resolution
H_2S	Cititech EZT3H	0-100 ppm	1% FS	0.5 ppm Resolution
CO_2	GasCard-NG	0-3000 ppm	2% FS	10 ppm Resolution

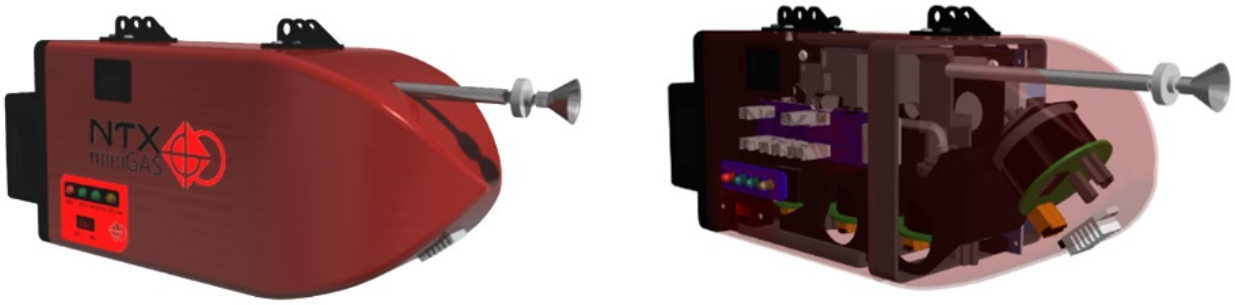

Figure 2. MiniGAS NTX System: Magmatic/Hydrothermal degassing monitoring payload for integration to unmanned aerial vehicles (UAV) and drones. System includes GPS based datalogger with telemetry for airborne, car or hand carried gas sampling, pressure, temperature, R= relative humidity and GPS sensors (T, P, RH% Lat., Long & Altitude); multiple single gas sensors: SO_2, H_2S, CO_2. Onboard data logging (microSD card), telemetry, USB antenna receiver, software, external switchable power on/off, status LEDs, two hot-swappable power supplies capability, external anchor support. Payload system has been successfully tested in Kilauea, USA; Alaska, USA; Solfatara, Italy, Vulcano, Italy; Turrilaba, Costa Rica; Poas Costa Rica; Masaya, Nicaragua. See following links:
Turrialba: https://www.youtube.com/watch?v=-EJzZnKS7g4
Masaya: https://www.youtube.com/watch?v=pMSiK9P2Y14
Poas: https://www.youtube.com/watch?v=kprEpvqTCIU

2.2 Mini Mass Spectrometer for Drones: UAS-miniMS-XPR3

The UAS-miniMS-XPR3 is miniature mass spectrometer design to be integrated into an unmanned aerial system (UAS) developed to be autonomous, compact and relatively light-weight for *in situ* chemical determination of the main components of atmospheric samples such as volcanic plumes, industrial plumes, leaks etc. using mid- lift drones and unmanned aerial vehicles (UAVs). This instrument is the last generation of miniature mass spectrometer systems developed by Dr. Diaz, with the aim of being carried on relatively small drones into harsh environments. It uses a commercial off the shelf (COTS) high pressure miniature quadrupole mass spectrometer with 2 mm radius rods from Inficon Inc., and it has 1-100 amu mass range, capable of detecting mostly any gas present from ppm to 100% concentration. Previous versions were first tested at Turrialba and Miravalles Volcanoes, Costa Rica in 2013 and La Solfatara Volcano, Italy in 2014 as backpack portable instruments carried into the field. The instrument was then ground tested at the La Solfatara -Vulcano during the 2015 campaign [Silvestri et al., 2016] to characterize the fumarolic sites where the measurements were conducted by hand carrying the instrument into the fumaroles.

The UAS-miniMS-XPR3 flying drone prototype uses a modified XPR3, with a reduction of total weight from its commercial version via shielding the electronic's box with aluminum foil. It also uses a a miniature pump system which consists of a turbo-drag and a scroll pumps from CREARE Inc, similar to the system used by Mars Science Lab (MSL) space probe, achieving 10-4 torr inside the vacuum chamber. It is controlled by a Fit-PC which records data onto its hard drive and sends the data via Wi-Fi with 100m range for real time data transmission. The system performs 1 scan/sec, detecting simultaneously H_2, He, H_2O, N_2, O_2, Ar, H_2S, CO_2, SO_2 molecules (and others) for volcanic emissions characterization and has an endurance of 4 hours. It weighs 7 kg including the onboard computer, the system battery, a red painted fiberglass waterproof cover and a light-weight internal structure that allows the instrument to be integrated on any UAV and deployed into volcanic environments (Figures 3 and 4).

Initial testing of the XPR3 spectrometer component was conducted using direct gas inlet to verify dynamic range and limit of detection (LOD). Targeted molecular gas species for volcanic plume analysis are: He, H_2, H_2O, N_2, O_2, Ar, CO_2, SO_2, and H_2S. Three calibration gases were used: Zero (0 ppmv UHP Ar), Test (1000 ppmv H_2, He, O_2, N_2, CO_2 in Ar background, and Span (10,000 ppmv H_2, He, O_2, N_2, CO_2 in Ar background.The spectra demonstrated the XPR3 spectrometer capability to achieve high dynamic range, very good linearity, and ppm limits of detection.. The system was also calibrated in the laboratory prior to the field deployment using a compact sample delivery system with flow and pressure control and three

certified NIST traceable calibration gas cylinders provided by AIRGAS/PRAXAIR in Costa Rica for zero-test-span calibration points. Calibrated SO_2 data taken by the field portable UAV-MS-XPR3 using 0, 5, 20, and 50 ppmv calibrated bottles achieved an LOD of 0.3 ppmv for SO_2 at 1 Hz scanning rate, less than 10% reading error, and less than 3% RSD.

The XPR3 –MS can operate in different modes, for quick volcanic plume for assessing chemical ratios (SO_2/ CO_2) and H_2S/ CO_2) it operates in single ion mode performing 1 scan / sec, detecting simultaneously H_2, He, H_2O, N_2, O_2, Ar, H_2S, CO_2 and SO_2. For an exploratory deployment to discover possible new species been emitted by the volcano, the MS is switched to full scan mode, taking 2 to 10 points per Da from 1 to 100amu. This takes more time (6-30 sec/scan) so it's only recommended when the drone can be flown in a fix position (hovering mode) to provide a better sample.

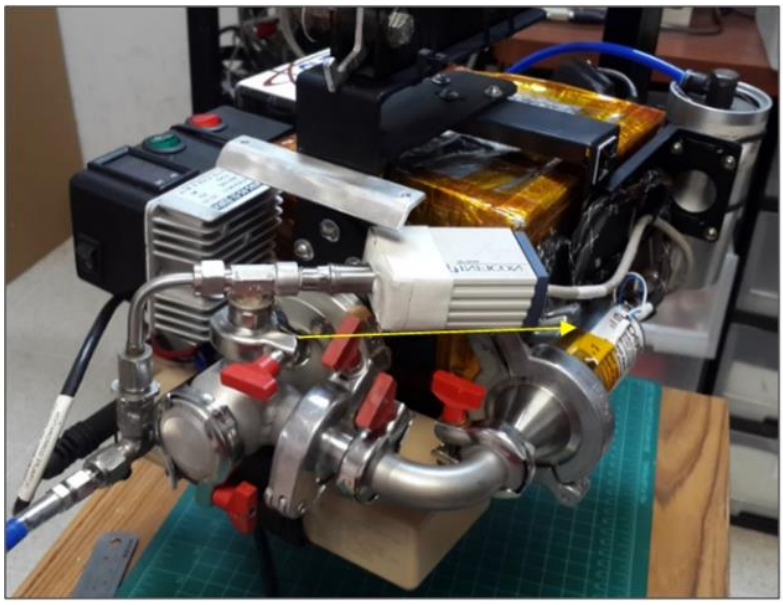

Figure 3. Internal UAS-miniMS-XPR3 prototype integration.

Figure 4. UAS-miniMS-XPR3 prototype integrated to S100+ drone for laboratory tests in Costa Rica.

The main characteristics of XPR3 are the following:

Parameter	Transpector XPR3 mass spectrometers extended pressure range residual gas analyzer
Mass range	1 to 100 Da
Max operating pressure	20 mTorr
Ion source	Two filaments ion source
Filaments	Yttria-coated iridium
Scan rate	1 Hz full spectra capabilities (fast measurement speed: 8 ms dwell)
Rods dimension	L = 18 mm poles r < 380 um
MDPP	6×10^{-12} Torr
Sensitivity	$>4 \times 10^{-3}$ A/Torr
Response time	Selectable from 8 to 128 ms (32ms usual configuration) per scan point
Cross sensitivity	None to fraction of peak depending on gas matrix (See MS fragmentation paterns) For volcanic gas matrix use deconvolution matrix [Diaz et al., Trends in analytical chemistry, vol. 21, no. 8, 2002]
Dynamic range	Six decade dynamic range
LOD	1-10 PPM depending on gas
Communication	RS 232/RS 485
Other characteristics	• Dual electron energy (40 or 70 eV) • Two ion chambers • Total pressure with separate chamber • Partial pressures with mass filter • Pirani interlock for filament protection • Off-axis micro-channel plate electron multiplier for up to 10 mTorr operation • Smallest COTS quadrupole foot print

2.3 Permanent Infrared Thermal Camera Network

The Thermal Infrared Permanent Network [TIRNet, Chiodini et al., 2007; Sansivero et al., 2013; Vilardo et al., 2015] managed by INGV, Osservatorio Vesuviano (INGV-OV) performs volcanic surveillance in the Campi Flegrei Caldera and consists of five stations which acquire thermal infrared frames of fumarole fields of the La Solfatara volcanic center (SF1, SF2, OBN, PSI and SOB stations; Figure 5). The IR frames are acquired and sent to a dedicated server in the monitoring room of Osservatorio Vesuviano in order to process them. The infrared sensors are FLIR SC645/655 cameras whose detector is a Focal Plane Array (FPA) uncooled microbolometer with a resolution of 640x480 pixels, with a spectral range of 7.5 - 14 μm, an accuracy of ± 2 °C and a thermal sensitivity of < 0.03°C @ +30°C.

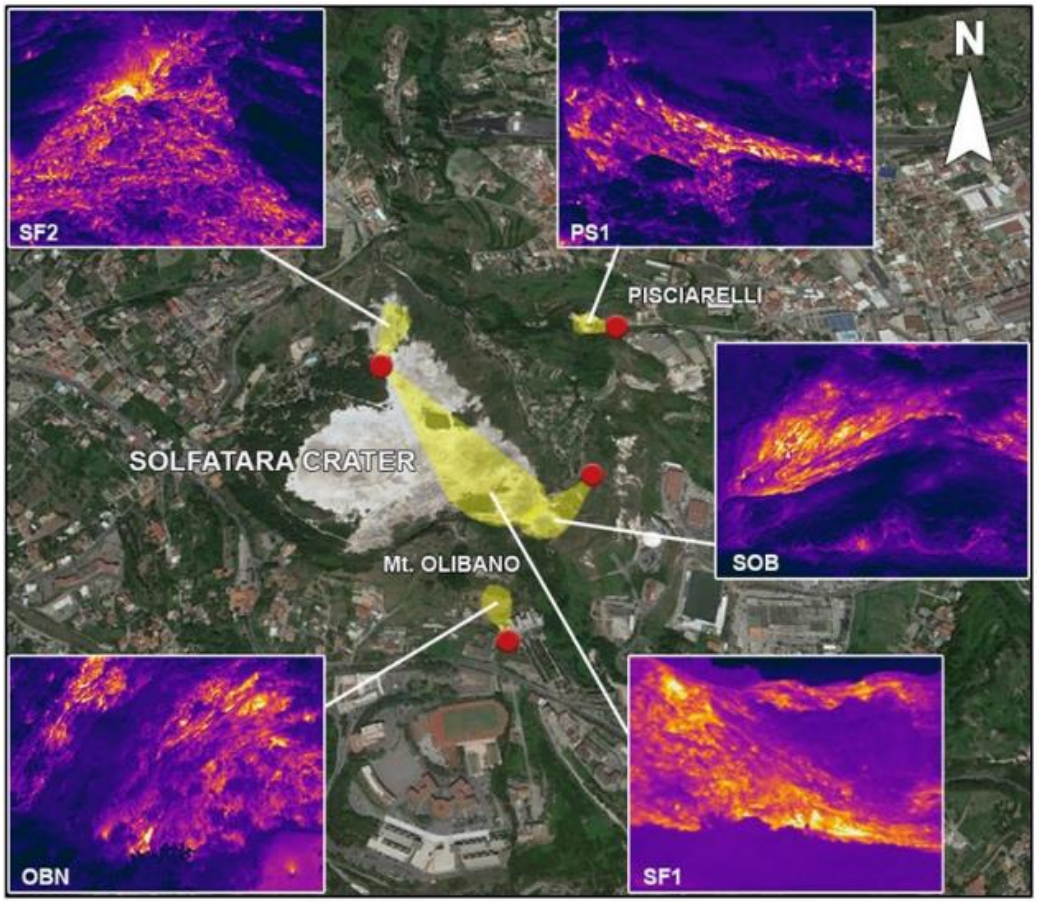

Figure 5. Location of the TIRNet permanent stations (red dots) and the investigated regions (yellow areas) with the IR frames at Campi Flegrei. SF1 = Solfatara Station 1; SF2 = Solfatara Station 2; SOB = Solfatara OB Station; OBN = Olibano Station; PS1 = Pisciarelli Station.

2.4 Mobile Thermal camera

The mobile thermal camera used for the surface temperature measurements by INGV-OV is a FLIR SC640. It has a resolution of 640 x 480 pixels, with a thermal sensitivity of 0.06° C (+30° C) and an accuracy of ± 2° C (or ± 2% of reading). As in the previous experiments [Silvestri et al., 2015], the thermal measures collected by TTM (Telecamere Termiche Mobili group of INGV-OV) were performed both in daytime and in nighttime in order to estimate the effects of solar irradiation over the acquired data that may interfere with thermal measurements. To perform this new set of measurements we focused on 3 large areas (Figure 6, Figure 7 and Figure 8) instead of single images shot at short distances. The thermal images have been composited using several single shots taken from some hundred meters of distance. In this way, each of them covers a large sector of the La Solfatara crater thus making them more suitable for the comparison with satellite thermal images.

The internal software of the FLIR camera allows us to correct each thermal shot for the effects of distance, atmospheric temperature and humidity. The latter two have been recorded by means of a thermo-hygrometer at the time of data acquisition. The single corrected shots have then been used to create the final panning images for which we performed a centile analysis in order to estimate the day/night differences on the acquired images.

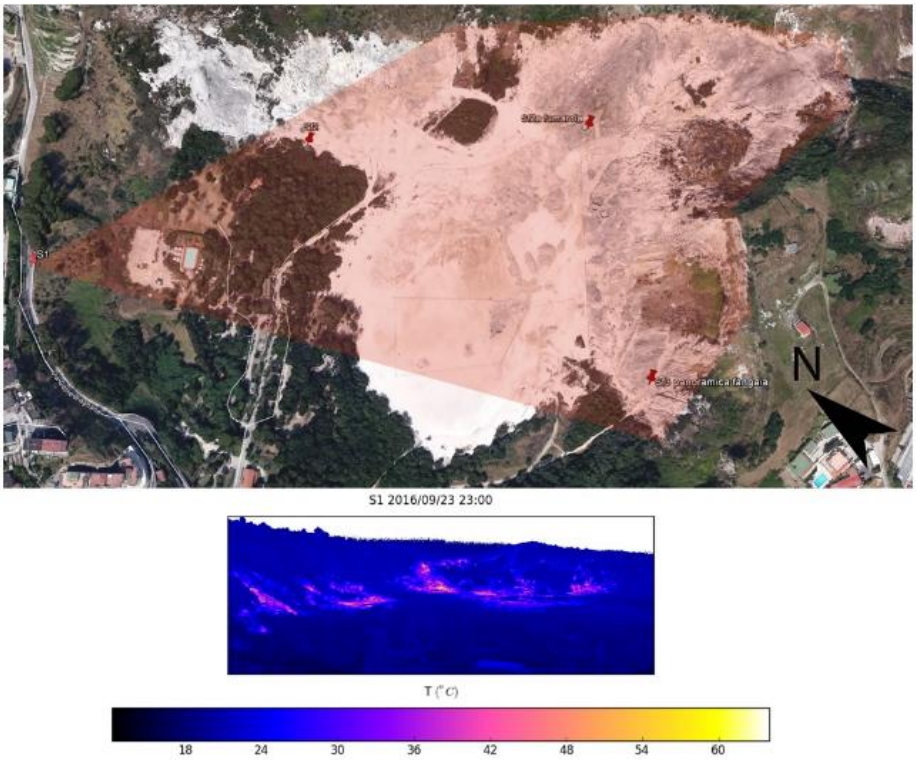

Figure 6. S1 measurement point position and an example of a panned image.

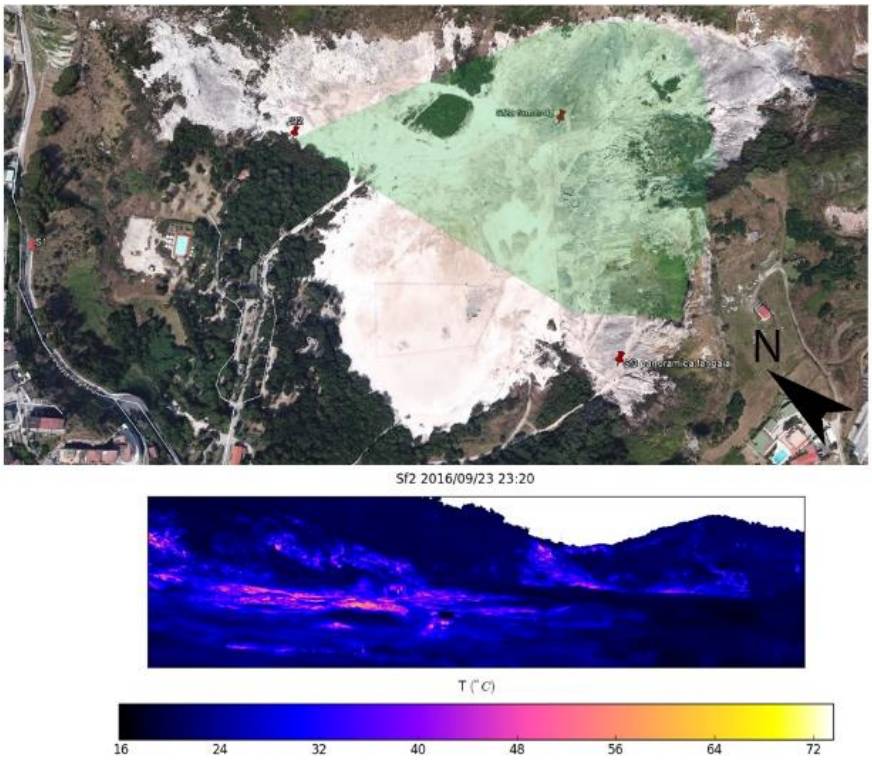

Figure 7. Sf2 measurement point position and an example of a panned image.

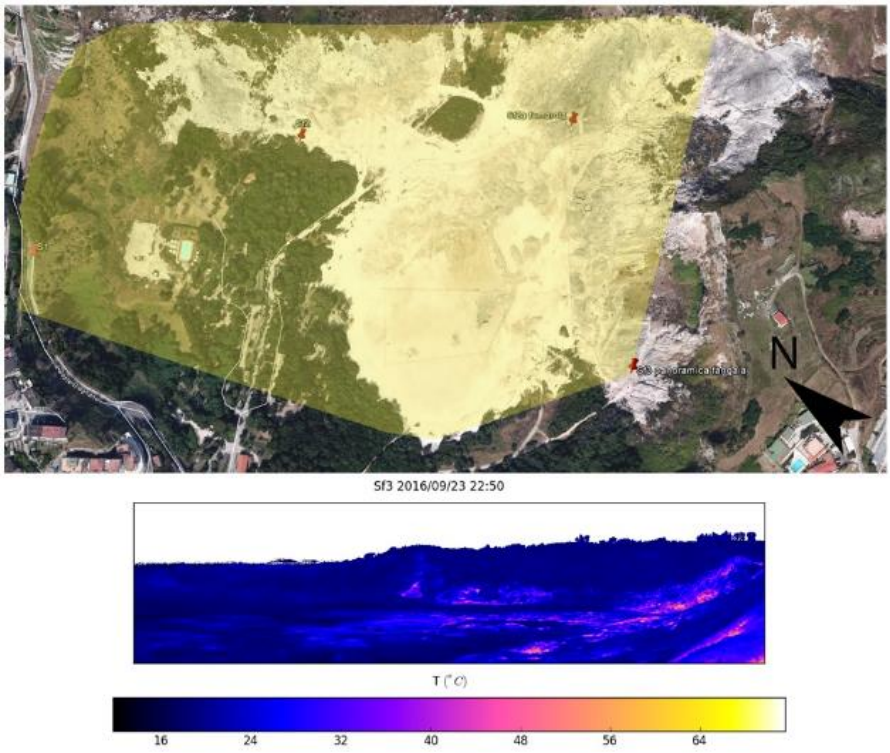

Figure 8. Sf3 measurement point position and an example of a panned image.

Along with these measurements, the surface temperatures have been collected with a Thermotecnix VISIR640 thermal camera of optical lab UF-8 (INGV-CNT). This camera provides clear images from a 640 × 480-pixel uncooled infrared sensor and a precise temperature measurement with a spectral range from 7.5 to 13 μm, an accuracy of ± 2 ºc (or ± 2% of reading) and a 60 mK thermal sensitivity. The measurements were performed in daytime and nighttime and covered the La Solfatara crater. In Figure 9, the sites where the measurements were collected are reported. The sites A, B and C represent three stations for the surface temperature comparison (Table 1).

Point	Latitude	Longitude	Description
A	40.82781	14.14158	soil
B	40.827204	14.14167	“Bocca Nuova” fumarole
C	40.82703	14.13938	“Fangaia”

Table 1. Sites coordinates for Thermotecnix VISIR640 thermal camera measurements.

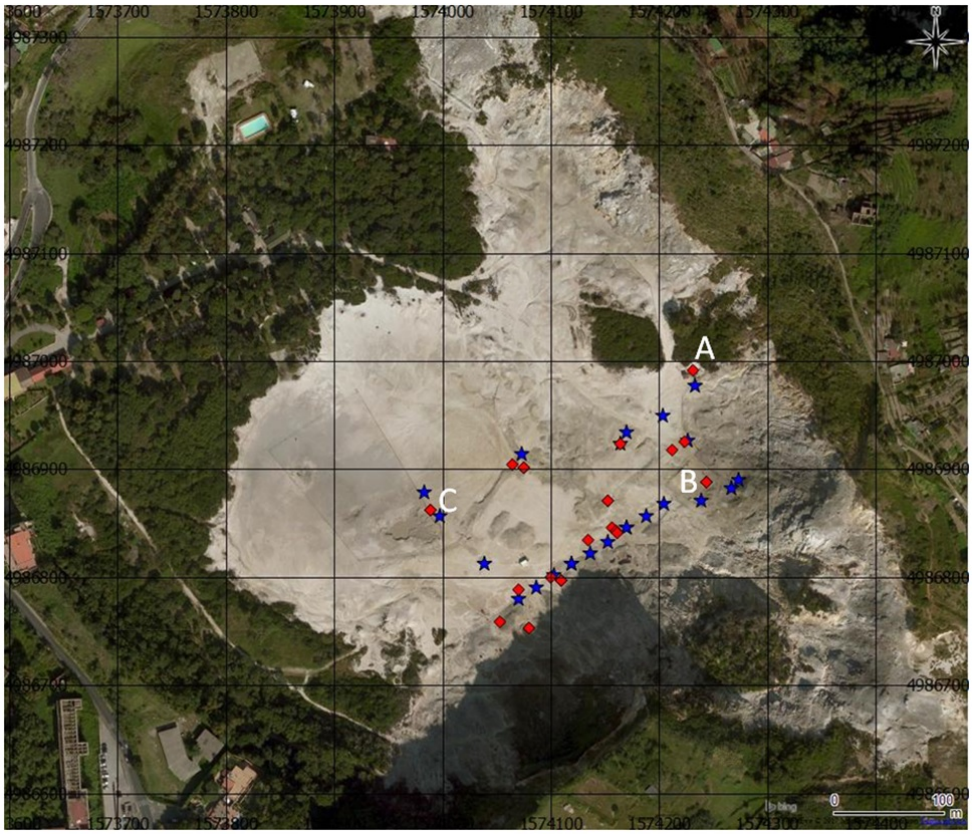

Figure 9. Sites of measures collected with Thermotecnix VISIR640 thermal camera. Stars represent the measurements collected on September 22, 2016 and diamond the measurements of September 23.

2.5 ASD Fieldspec

Analytical Spectral Devices [ASD, 2002] FieldSpec Pro FR portable spectroradiometer (Figure 10) permits the detection of individual absorption features due to specific chemical bands in a solid, liquid or gas state. Detection is dependent on the spectral range, spectral resolution, and signal-to-noise of the spectrometer (parameters that describe the instruments capability), the abundance of the material and the strength of absorption features for that material in the wavelength region measured.

Three separate spectrometers cover the 350-2500 nm spectral range. The first one operates between 350 and 1000 nm, with a spectral resolution (Full Width at Half Maximum, FWHM) of approximately 3 nm and a sampling step of 1.4 nm; the other two cover the region from 900 to 1850 nm and 1700 to 2500 nm respectively. The sampling in these regions is every 2 nm and the resolution varies between 10 and 11 nm. Measurements were made directly with the fiber-optic cable, which has a field of view of 25°. Data storage, visualization and calibration are performed in real time by dedicated software on a personal computer connected to the instrument (Figure 10).

During the field campaign, our team collected ground-truth spectral data, acquiring reflectance signatures of samples from sites all around the La Solfatara crater (Table 2, Figure 10) which showed different mineral and vegetative alterations.

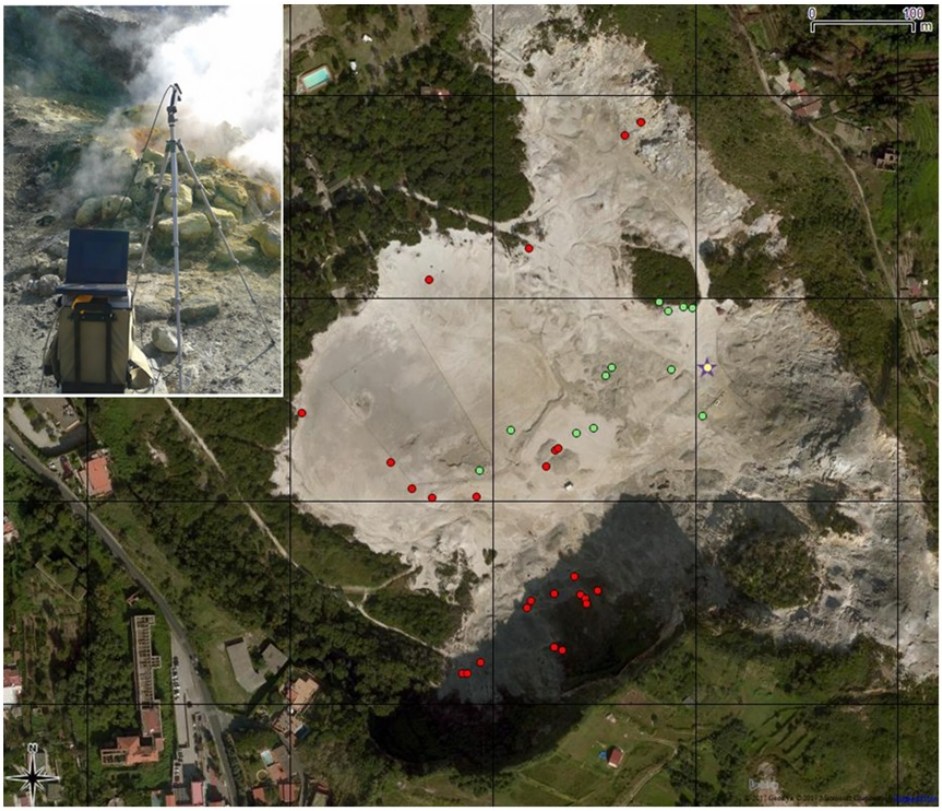

Figure 10. ASD FieldSpec Pro FR portable spectroradiometer set upped for the *in situ* acquisition (in the box) and sites of measurements collected with the instrument (red - 22nd of September 2016, green - 23rd of September 2016). In the figure the meteo station is represented with the star.

Site #	Latitude (°)	Longitude (°)	Brief description
1	40.82545	14.13922	Pyroclastic deposits (mainly trachytic) near Belvedere
2	40.82545	14.13926	Pyroclastic deposits (mainly trachytic) near Belvedere
3	40.82553	14.13937	Pyroclastic deposits (mainly trachytic) with traces of sulfur near Belvedere
4	40.82563	14.14004	Dry grass
5	40.82561	14.14010	Background soil behind sample #4
6	40.82594	14.13983	Debris with argillic alterations (presence of diffuse degassing)
7	40.82588	14.13979	Debris with argillic alterations (presence of diffuse degassing)
8	40.82599	14.14003	Green shrub, partially chloritic
9	40.82598	14.14026	Dark bare soil (background of sample #8)
10	40.82595	14.14031	Green healthy grass
11	40.82591	14.14032	Dry grass
12	40.82610	14.14023	Green healthy shrub
13	40.82602	14.14041	Dry grass
14	40.82682	14.13997	Solfatara basement, argillic alterations
15	40.82688	14.14003	Solfatara basement, argillic alterations with sulfate hydrates and sulfur
16	40.82696	14.14007	Solfatara basement, argillic alterations
17	40.82664	14.13934	Solfatara basement, argillic alterations
18	40.82661	14.13895	Solfatara basement, argillic alterations
19	40.82670	14.13875	Solfatara basement, argillic alterations flooded by Fangaia mud
20	40.82688	14.13858	Solfatara basement, argillic alterations flooded by Fangaia mud
21	40.82721	14.13780	Solfatara basement, argillic alterations in proximity of the vegetated area (east)
22	40.82808	14.13891	Solfatara basement, argillic alterations near vegetation (north)
23	40.82830	14.13981	Solfatara basement, argillic alterations near vegetation (north)
24	40.82906	14.14066	Altered trachytic deposits with diffuse fumarolic activity near Stufe
25	40.82917	14.14087	Green shrub, partially chloritic, near Stufe

Table 2. The 25 sites sampled in this field campaign of 22nd September, with geographic coordinates (WGS84) and a brief description of the target.

2.6 Satellite data

During the La Solfatara field campaign, two sets of satellite data were considered: Landsat 8 (NASA and USGS) and ASTER (NASA, Japan's Ministry of Economy, Trade and Industry (METI), and Japan Space Systems). For the satellites featured we refer to Silvestri et al., [2015] and to specific web sites (Landsat 8 https://landsat.usgs.gov/landsat-8 and ASTER https://asterweb.jpl.nasa.gov). The aim of using the satellite data was to obtain a surface temperature map covering the whole La Solfatara volcano by considering the ASTER's five thermal infrared channels (B10 - B14, covering the thermal range from 8.125 to 11.65 micron) and the band B10 (10.60–11.19 micron) for Landsat 8, infact thermal infrared bands are particularly useful for detecting thermal anomalies. Unfortunately, the thermal data could not be analyzed because of cloud coverage. For this reason, considering the low variation of temperature in September, as in Figure 11, and in order to compare the surface temperature measurements obtained by means of satellite data and the Permanent Infrared Thermal Camera Network described in paragraph 2.3, we analyzed the ASTER acquisition of September 6, 2016 and the Landsat 8 acquisition of September 7, 2016. For these satellites, we analyzed the nighttime acquisitions in order to remove the contamination of reflected solar radiation that produces an apparent surface temperature higher than the actual one. At night, this contamination is not present and the data more clearly differentiates the temperature difference between the crater and the surroundings.

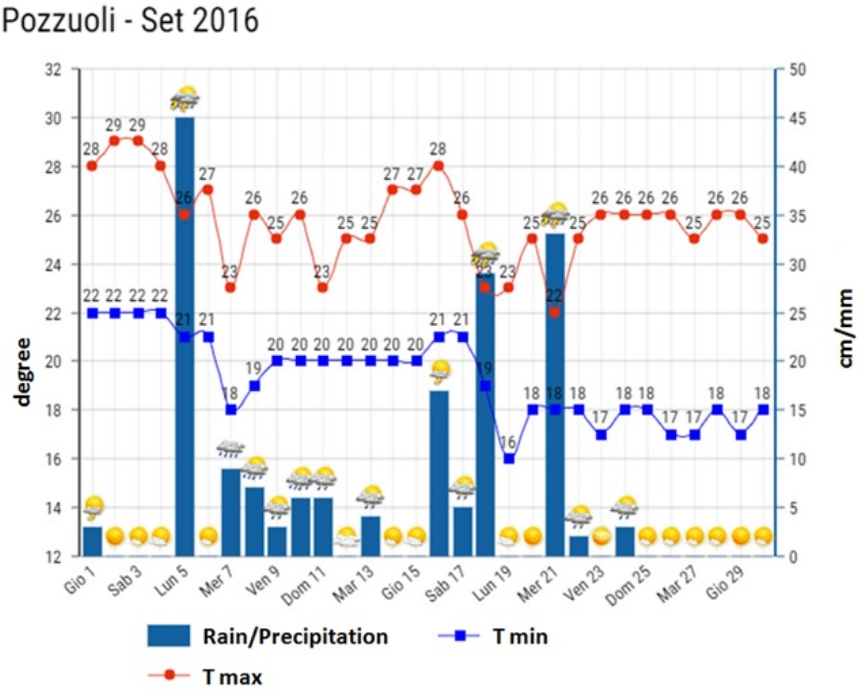

Figure 11. Minimum (blue), maximum (red) temperature and precipitation measured in the month of September 2016 (https://www.3bmeteo.com/meteo/pozzuoli/storico/201609).

2.7 UAV (Unmanned Aerial Vehicles)

During the campaign the following UAVs were used:

Model	Max. Payload	Autonomy	Purpose
Quadcopter - DJI Phantom Vision plus 2	600 grams	6 min	Photogrammetry
Octocopter - ITALDRON E-EPIC 8HSEMAX	10 kg	25 min	Gas Sampling

The DJI Phantom Vision 2 Quadcopter has been already used in the 2014 and 2015 Solfatara campaigns and its features are reported in Silvestri et al. [2015; 2016]. This drone has been used during the campaign in order to collect photos and videos. The E-EPIC 8 Italdrone Octocopter has been used for gas sampling with MiniGAS and UAS-miniMS-XPR3 instrument, offering the possibility to analyze gases and

to produce real time 3D gas concentration maps. The Octocopter has a carbon fiber structure, up to 10 kg Payload, redundant FCU/IMU and GPS, with a total weight takeoff of 22 kg and a wind resistance at 12 m/s. The UAS-miniMS XPR3 with its weight of 7kg has been mounted on octocopter and the gas sampling has been collected during flying over the fumaroles, allowing a safe acquisition of volcanic emissions data (Figure 12).

Figure 12. MiniGAS NTX (left) and UAS-miniMS XPR3 (right) mounted on E-EPIC 8 Italdrone Octocopter.

3. Preliminary results

3.1 Calibration Lab Test

To prepare and calibrate the gas instruments used for the in-situ measurements, a series of gas standards with certified concentrations of the target gases (SO_2, H_2S and CO_2,) were used at the chemical laboratory of the INGV-OV in Naples before the deployment. Each voltage and ion intensity trace was calibrated to the proper concentration in parts per million. The gases used for calibration were:

Bottle 1:
CO_2 29.83%; 02 14.41%; Ar 0.93%; CH4 0.196 %; H_2S 34.0 ppmv, N2 filled

Bottle 2:
CO_2 8.66%; He filled

Bottle 3:
CO_2 0.836 %; CH4 44.8 ppmv; N2 filled

Bottle 4:
CO_2 1004 ppm; N2 filled

Figure 13 shows a calibration trace of the UAS-MS–XPR3 instrument exposed to Zero, Bottle 1 Gas and Zero Gas again at 1 scan/sec rate in single ion mode.

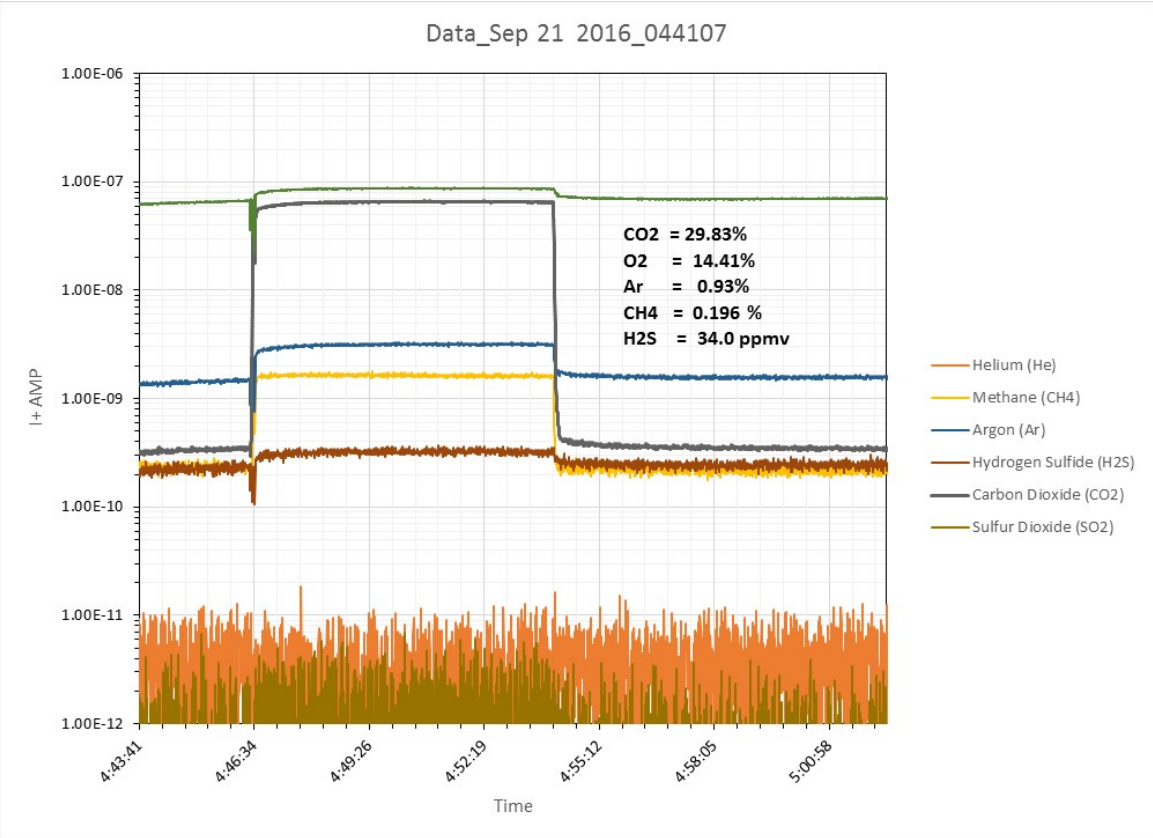

Figure 13. Calibration trace of the UAS-MS–XPR3 instrument.

3.2 MiniGAS NTX

The NTX MiniGAS was deployed at the La Solfatara 2016 campaign using the Italdrone E-EPIC8 Octocopter as its UAS platform and flying low over the fumarolic sites or hand carried to perform ground surveys. Figure 14 shows the payload already mounted below the Italdrone. A 1.5 m tube was added to collect sample outside the turbulence and downward air draft caused by the multicopter propellers.

Figure 14. The NTX MiniGAS instrument integrated to Italdrone Octocopter at La Solfatara 2016 deployment.

The MiniGAS recorded the gas concentrations along with GPS geolocation data to generate 3D concentration profiles of CO_2, H_2S and SO_2 across the area covered by the instrument during the deployment. Every generated profile has its own color scale regarding the maximum and minimum concentration measured where the red color indicates the higher concentration measured on that particular monitoring and the dark green color indicates the minimum. These plots were then superimposed into Google Earth 3D maps to create a trace of each gas concentration. In the figures that follows (Figure 15 - Figure 18) the main results are shown, focusing on CO_2 (Blue Trace) and H_2S (Red trace). There was not any considerable amount of SO_2 measured during the deployment as shown in Figure 15 (green trace). At each deployment a Zero gas exposure was done for at least 1 minute using CO_2 and Sulphur filters attached to the intake, therefore the signal on all gases went to zero.

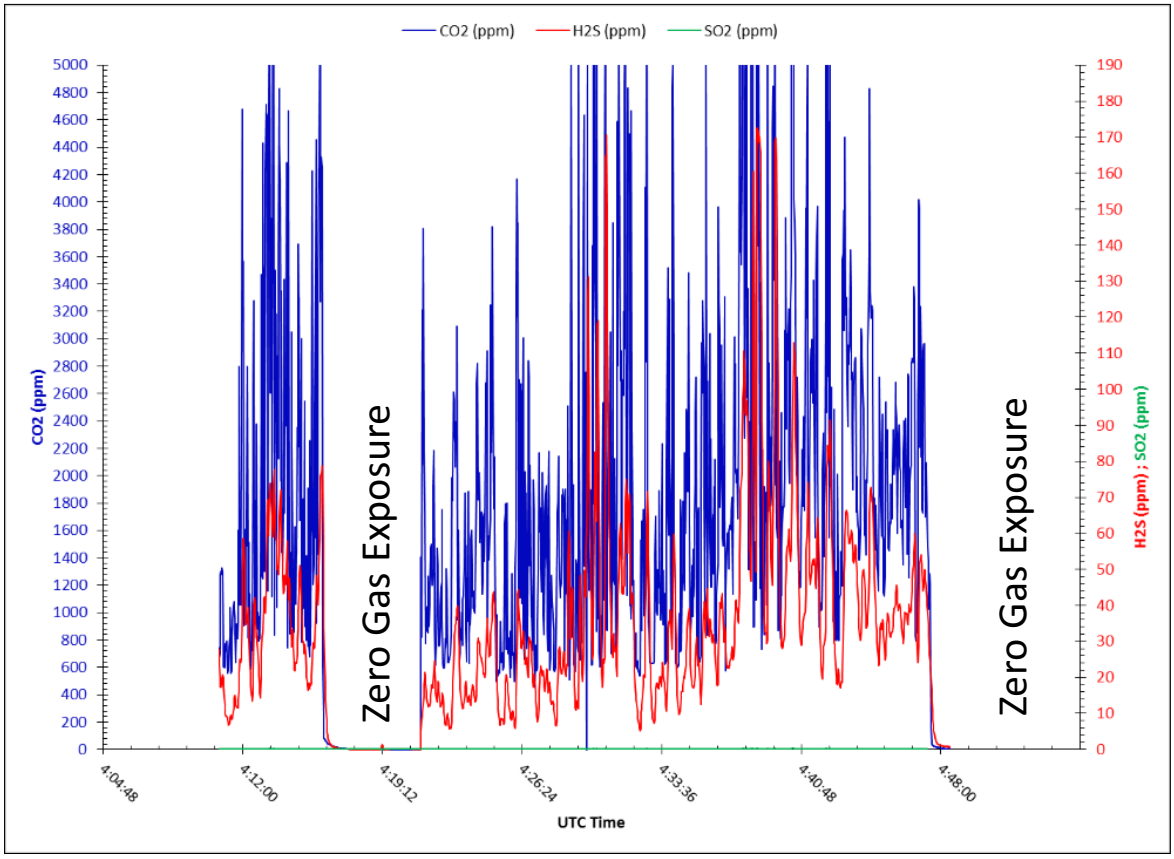

Figure 15. MiniGAS NTX: CO_2, H_2S and SO_2 concentrations during UAV flight of September 22, 2016.

Figure 16Figure 16 and Figure 17 shows the H_2S and CO_2 3D plots for UAV flights performed on September 22nd and 23rd, 2016 using the MiniGAS onboard the Italdrone. High Concentrations of CO_2 (up to 5500ppm) and H_2S (up to 190 ppm) were measured during the flights. The concentration values may have been higher due to the fact that the gases saturated the CO_2 and H_2S sensors in some instances.

Figure 18 again shows also the CO_2 and H_2S concentration of the La Solfatara site when conducting a ground survey walking with the instrument at hand level. Background levels of CO_2 were measured on the order of 400ppm and concentrations also high (above 5000ppm for CO_2 and 200ppm for H_2S) were measured during the ground survey.

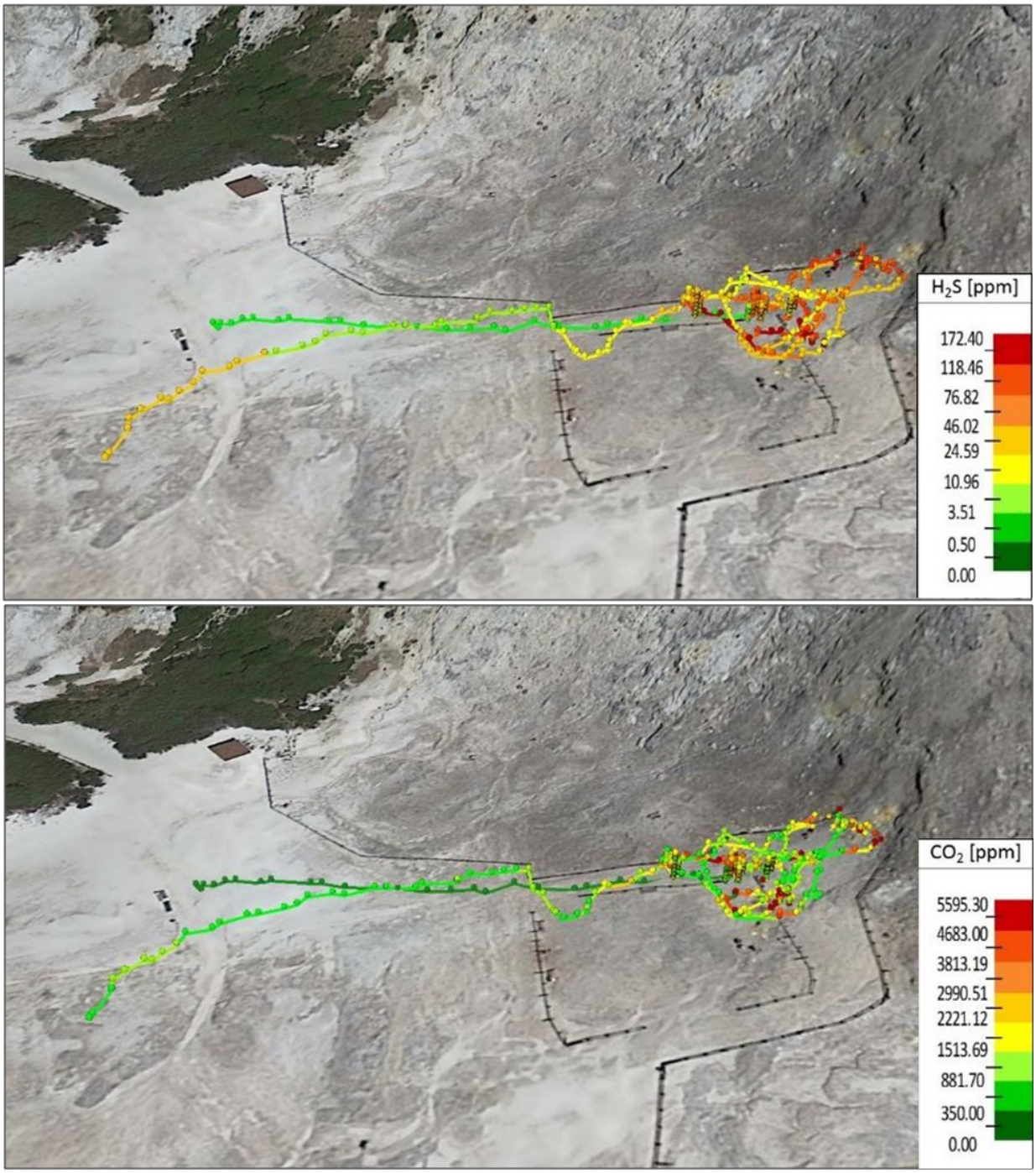

Figure 16. MiniGAS NTX 3D concentration H_2S (top) and CO_2 (bottom) profile after UAV flight of September 22, 2016.

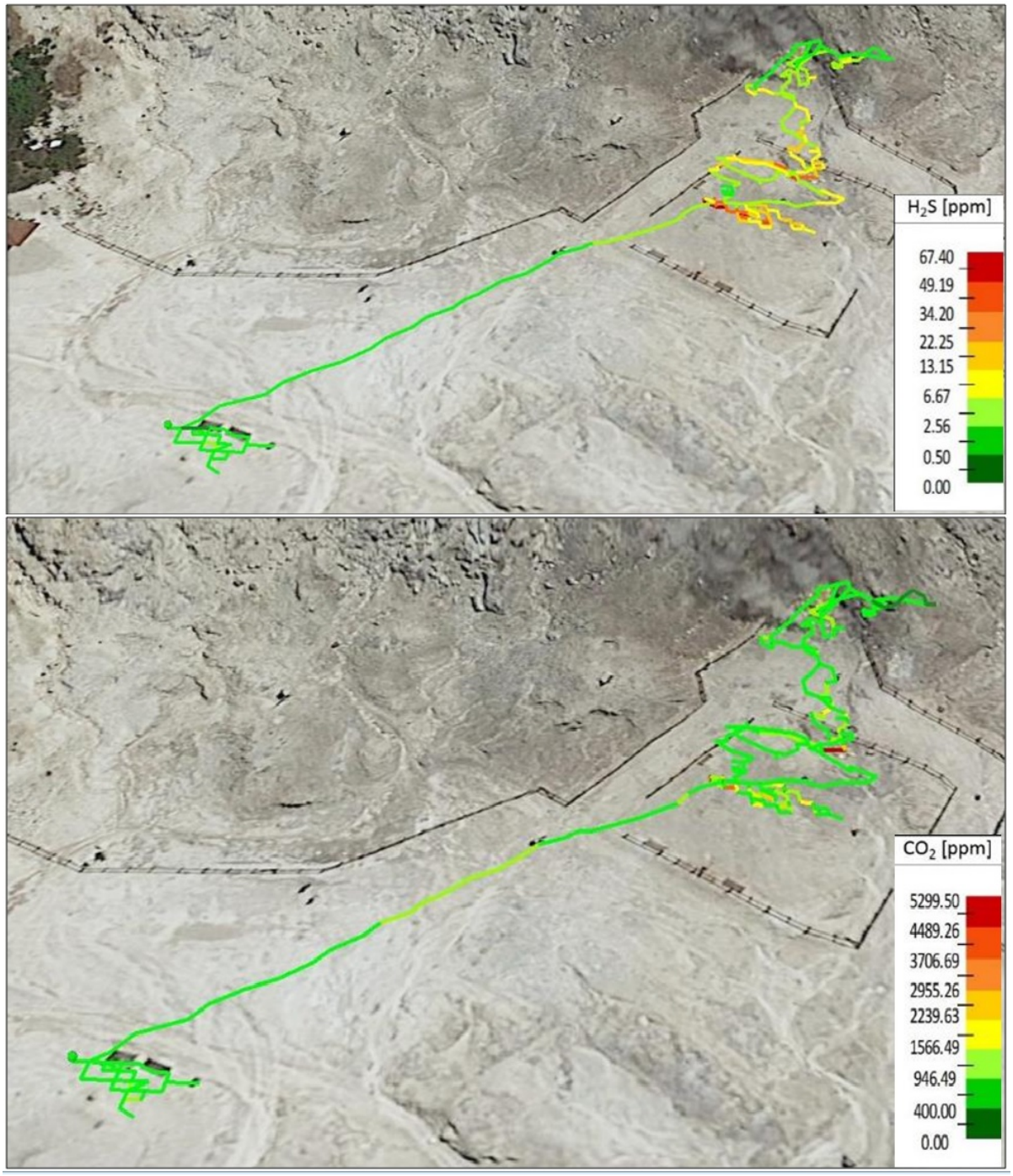

Figure 17. MiniGAS NTX 3D concentration H_2S (top) and CO_2 (bottom) profile after UAV flight of September 23, 2016.

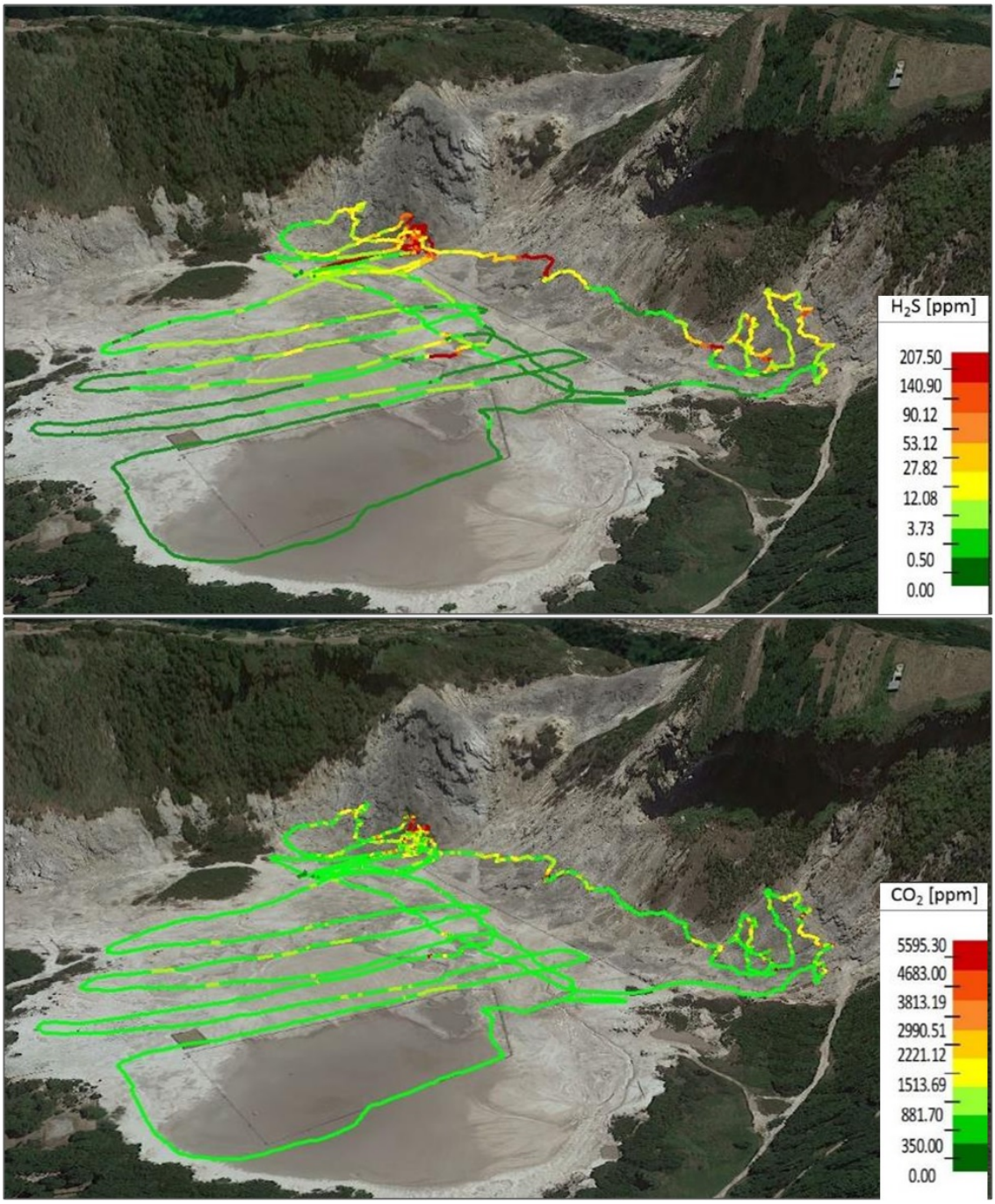

Figure 18. MiniGAS NTX 3D concentration H_2S (top) and CO_2 (bottom). Walk sampling on September 23, 2016.

3.3 UAS-miniMS-XPR3

The UAS-miniMS-XPR3 prototype was also deployed during the La Solfatara 2016 campaign using the Italdrone E-EPIC8 Octocopter and flying tethered at low altitudes over the fumarolic sites.

Figure 19 shows the payload ready to be mounted on the side of the Italdrone and the deployment team during the test flight and Figure 20 shows the system flying on top of "Bocca Nuova" and "Bocca Grande" fumaroles at La Solfatara. The same 1.5 m tube was used to collect sample outside the turbulence and downward air draft caused by the octocopter propellers as had been done with the MiniGAS. To our knowledge, this was the first time a miniature mass spectrometer was used to conduct multicopter drone based measurement of volcanic plumes.

Figure 19. UAS-MiniMS-XPR3 next to INGV's Italdrone Octocopter.

Figure 20. UAS-MiniMS-XPR3 flying over La Solfatara "Bocca Nuova" and "Bocca Grande" fumarole onboard INGV's Italdrone Octocopter.

Figure 21 shows the results obtained with the UAS-miniMS XPR while flying over the fumaroles at La Solfatara. The test lasted 25minutes with Zero gas exposed at the beginning of experiment and 7 minutes into the flight test. The drone was elevated to 30 m for the first airborne test, the dropped to the ground for service and then flown again for the second airborne sampling.

The data show a consistent CO_2 trace with high concentration peaks (above 10k ppm) when sampling the volcanic plume and no saturation at high concentration which is an improvement over the MiniGAS results. The data also show zero SO_2 concentration which is consistent with MiniGAS data and the results obtained from continuous monitoring by the Osservatorio Vesuviano. The H_2S trace shows that this gas is present in the sample (when switching between the Zero gas and the airborne sample) but it lacks the peaks observed in the CO_2 trace, so there is a degradation of this gas when it is injected into the mass spectrometer. The calibration gases showed a sensitivity to H_2S as per the miniMS at the lab, therefore the issue likely happened when the instrument was integrated into the UAS drone. Unfortunately, only one test flight was possible since the turbo drag pump failed after the flight test, with no time to repair it prior the end of the deployment. The different level in the zero signal shows the background level changing which is an indication of a problem with the pump or inlet that later transformed into a pump failure. More testing is been planned to resolve this issue. The unit is working well at the lab again and our team is preparing for the 2017 campaign to test an improved version.

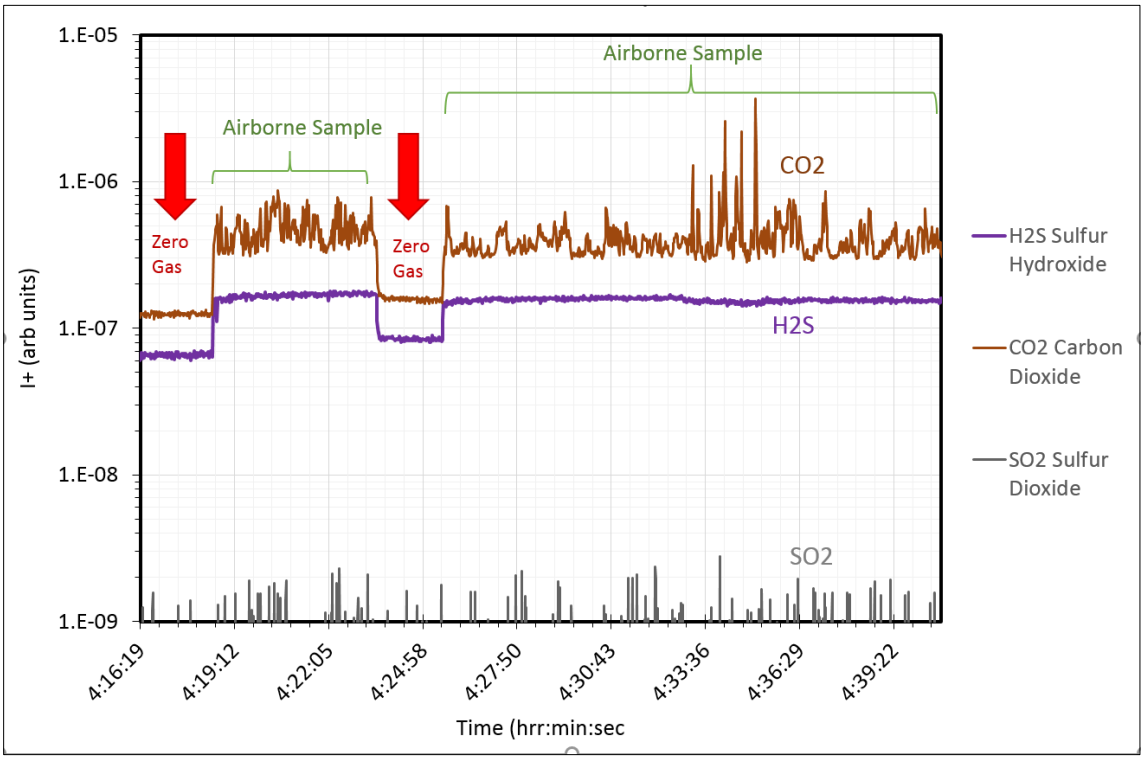

Figure 21. UAS-MS XPR3 Flight test at La Solfatara. Italdrone Platform. CO_2, H_2S and SO_2 profiles of September 22, 2016.

3.4 Permanent Infrared Thermal Camera Network and Satellite data

With the aim to compare the TIRNet ground data to the Landsat-8 and ASTER satellite images, extra-acquisitions of the TIRNet were programmed to coincide with the time of the satellite passages over the Campi Flegrei area. The TIRNet stations involved were SF1, SF2, OBN and SOB (Figure 5). The comparison between satellite and ground images was possible only after a geometric correction of TIRNet frames which permitted the draping of these frames over a DSM (Digital Surface Model). A visibility analysis of each station by using FoV (Field of View) values of TIRNet cameras (Figure 22) allowed for the rectification and the geo-referencing of the frames in the UTM WGS84 System (Figure 23). This procedure was accomplished in the ESRI ArcGIS software environment.

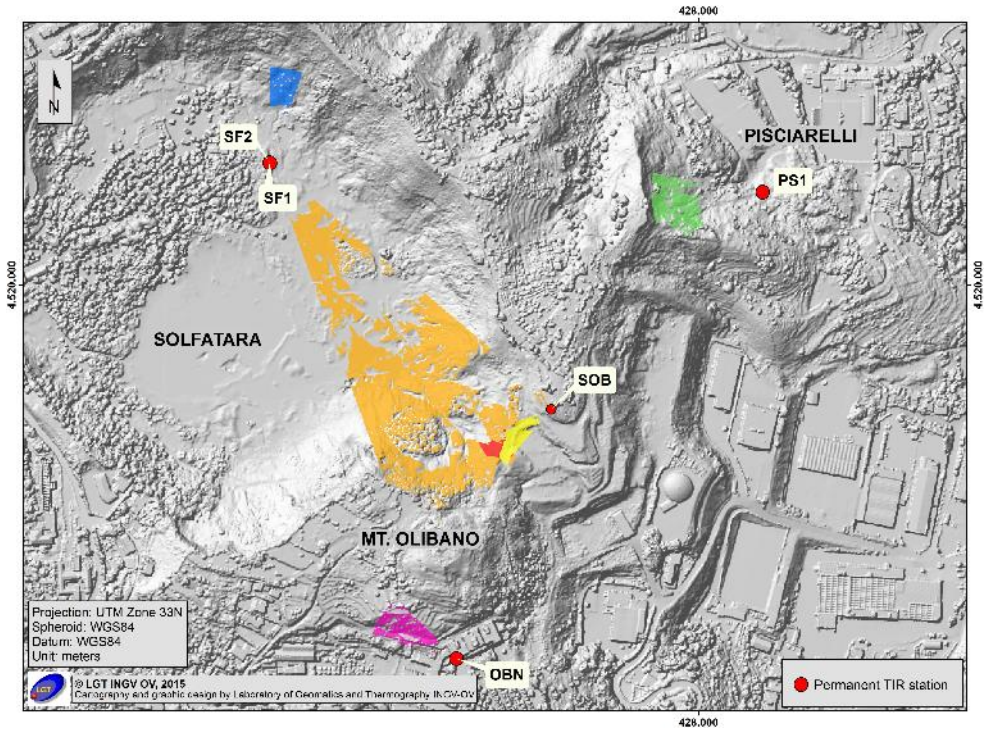

Figure 22. Location and visibility analysis of TIRNet stations in the Campi Flegrei area.

As the resampling of the satellite data results in a resolution of 30x30 m, a regularly-spaced 30x30 m grid was created to compare the temperatures of satellite images and TIR ground images. By grouping 30x30 m cells which contain data of TIRNet frames, several polygons were created (Figure 23 b).

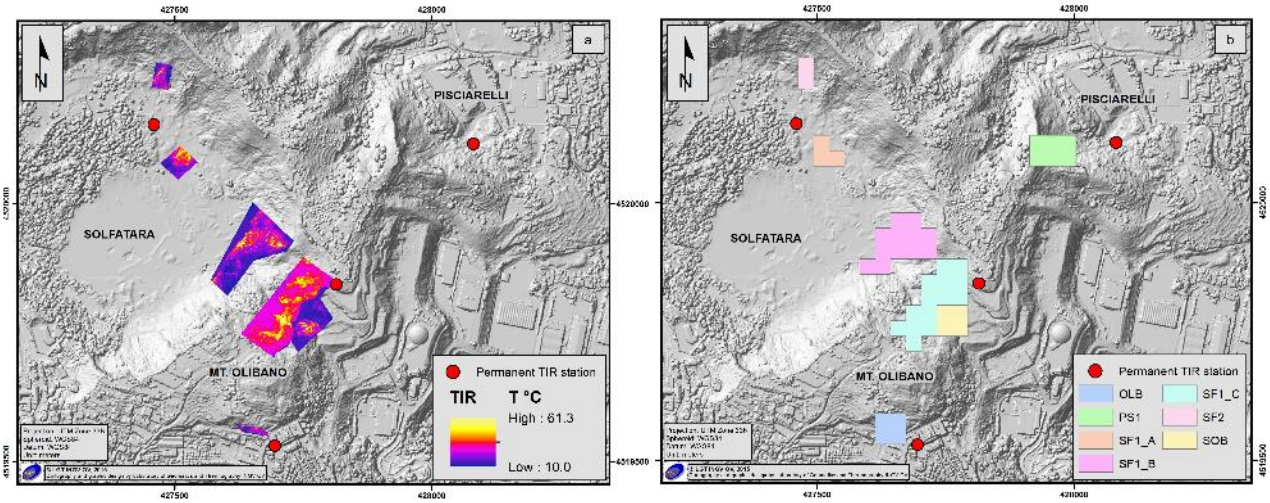

Figure 23. a) Draped and georeferenced TIR images of SF1, SF2, OBN and SOB stations. The image of SF1 Station is split into three coherent parts with different focal geometry (SF1_A/B/C); b) polygons obtained by grouping cells containing data from TIRNet stations. SF1_A/B/C= Solfatara Station 1; SF2 = Solfatara Station 2; SOB = Solfatara OB Station; OBN = Olibano Station; PS1 = Pisciarelli Station.

In Figure 24 the surface temperature obtained using the ASTER and Landsat 8 data is shown. The TIR channels of satellite data (i.e., radiance at the sensor) have been processed by a means code written in the IDL/ENVI image-processing environment (Exelis Visual Information Solutions, Inc. USA, www.exelisvis.com), implemented in three steps:

1) from the original cloud free data format (Level-1), the geo-referenced images are obtained using ENVI batch commands and the radiance at the sensor are automatically produced;
2) an atmospheric correction has been applied to the satellite data. The atmospheric and topographic corrections of remote sensing images are very important to obtain reliable values for many surface parameters (reflectance, vegetation indexes, ocean chlorophyll maps, temperature, etc.) but represent a very difficult preprocessing step. For these EO data, we have used the "CIRILLO" atmospheric correction tools [Musacchio et al., 2007]. Information on the atmospheric profiles corresponding to the time of the satellite overflights are provided by University of Wyoming and atmospheric temperature, pressure and humidity are considered;
3) Surface temperature maps are produced following Gillespie et al. [1998] for ASTER data and Barsi et al. [2003] for Landsat 8.

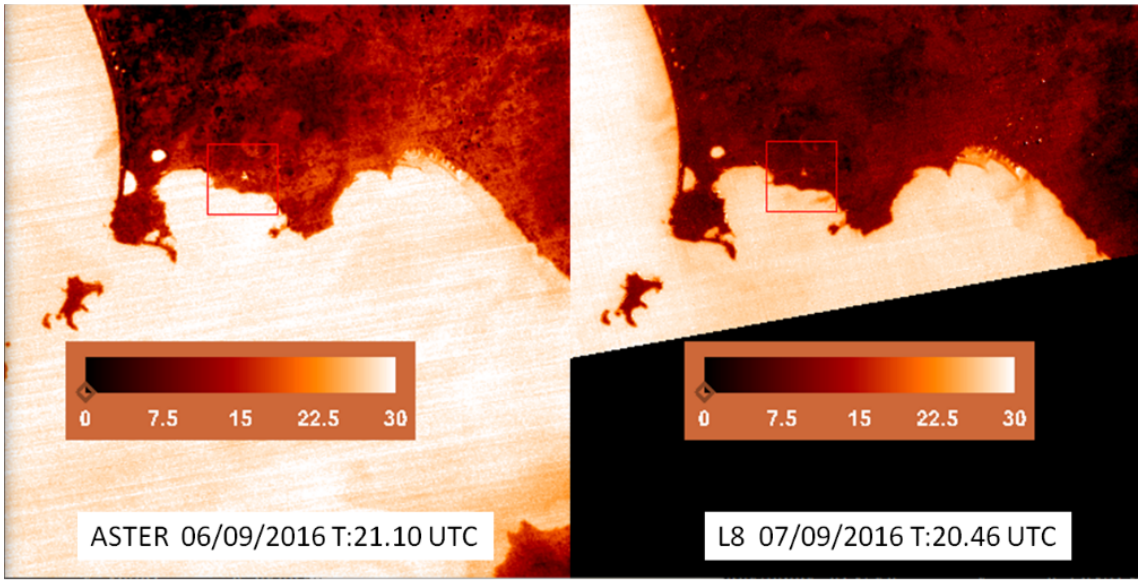

Figure 24. Surface temperature map (°C) for the Flegreian area: ASTER acquisition (left) and Landsat 8 acquisition (right).

Figure 25 a) and b) show the polygons described in Figure 23 a) overlaying the ASTER and Landsat-8 satellite frames acquired respectively on 2016.09.06 (21:10 UTC) and 2016.09.07 (20:46 UTC) respectively.

This process has allowed us to make comparison between satellites and TIRNet temperature data inside the selected polygons and the observed values are reported in Table 3.

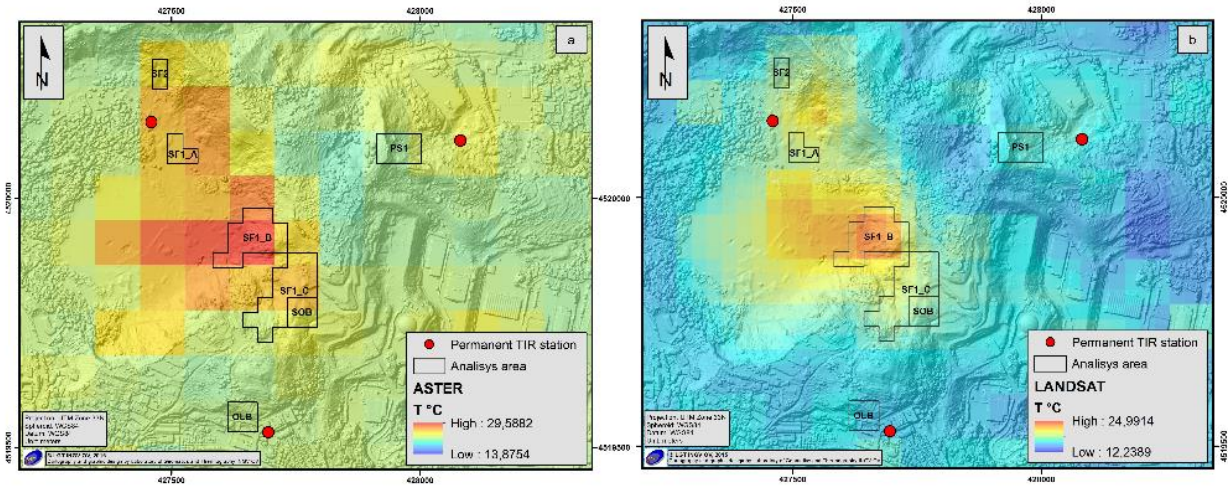

Figure 25. Aster (a) and Landsat-8 (b) satellite images and the polygons enclosing data of TIRNet stations.

DATE	STATION	T MIN(°C)	T MAX (°C)	T AVERAGE (°C)	IMG TYPE
20160906	SF1_A	25.46	26.83	25.92	ASTER
20160906	SF1_A	15.50	40.70	22.16	TIRNet
20160907	SF1_A	18.32	18.71	18.56	LANDSAT
20160907	SF1_A	13.50	36.80	18.43	TIRNet
20160906	SF1_B	24.99	29.15	28.18	ASTER
20160906	SF1_B	17.50	60.70	25.45	TIRNet
20160907	SF1_B	20.47	23.07	22.20	LANDSAT
20160907	SF1_B	13.70	58.50	21.45	TIRNet
20160906	SF1_C	22.53	25.88	24.85	ASTER
20160906	SF1_C	6.70	50.80	23.62	TIRNet
20160907	SF1_C	17.02	19.65	18.36	LANDSAT
20160907	SF1_C	7.50	46.20	20.30	TIRNet
20160906	SF2	24.67	24.67	24.67	ASTER
20160906	SF2	17.90	72.10	26.90	TIRNet
20160907	SF2	17.63	17.92	17.78	LANDSAT
20160907	SF2	15.30	61.30	23.37	TIRNet
20160907	SOB	17.14	18.00	17.52	LANDSAT
20160907	SOB	13.30	59.10	19.10	TIRNet
20160907	OBN	15.58	16.27	15.94	LANDSAT
20160907	OBN	12.90	61.30	19.41	TIRNet

Table 3. Temperature values observed both in TIRNet and satellite frames.

3.5 Mobile Thermal camera

We shot two panning images during daytime and two images at night for the points SF2 and SF3, while for the point S1 we preferred to only shoot nighttime images. For each panning image we calculated a set of centiles in order to understand in detail the distributions of hot and cold pixels and how they evolve during night and day (Figure 26, Figure 27 and Figure 28).

Centiles for the SF2 and SF3 pannings show a clear difference in the distributions between nighttime and daytime where the latter are strongly influenced by solar radiance and weather conditions. On the contrary, the nighttime shootings show quite stable distributions and are, for this reason, the best possible conditions to shoot medium to long distance thermal images.

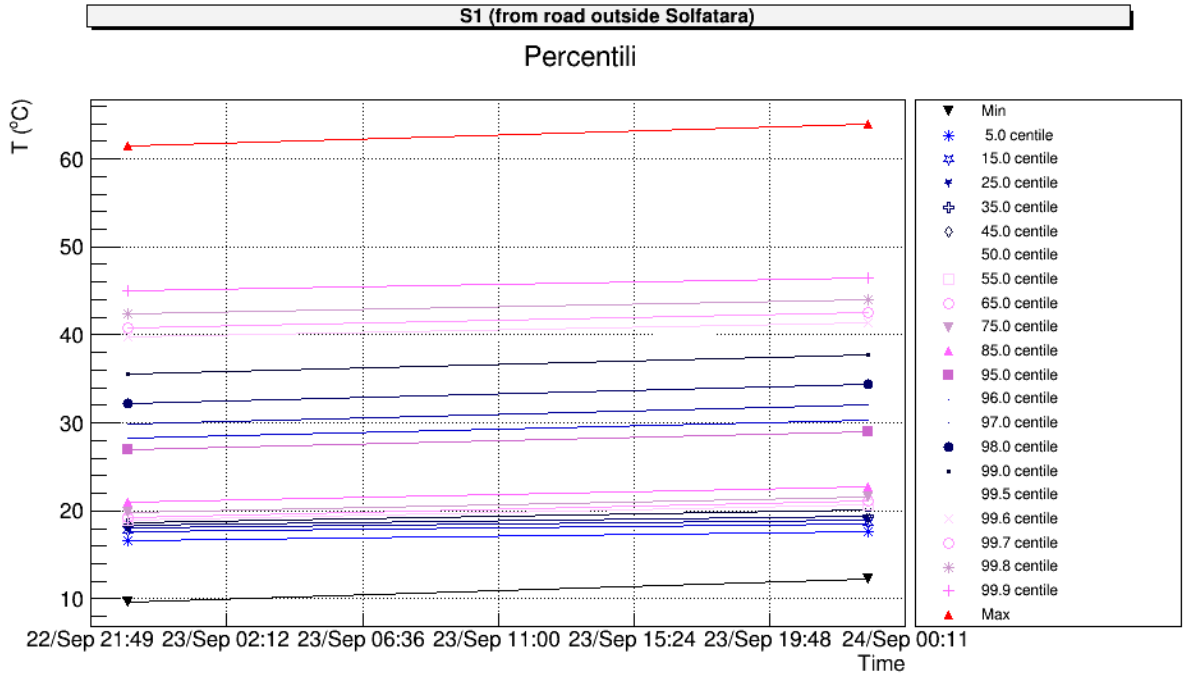

Figure 26. Centiles distribution of the S1 panning images.

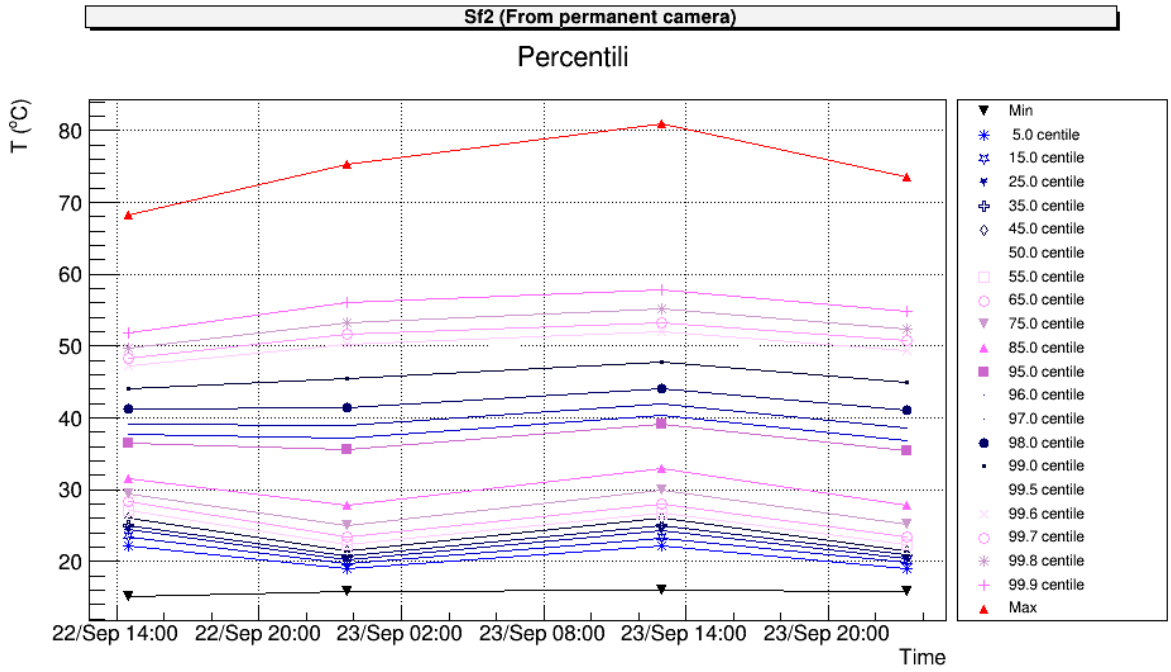

Figure 27. Centiles distribution of the Sf2 panning images.

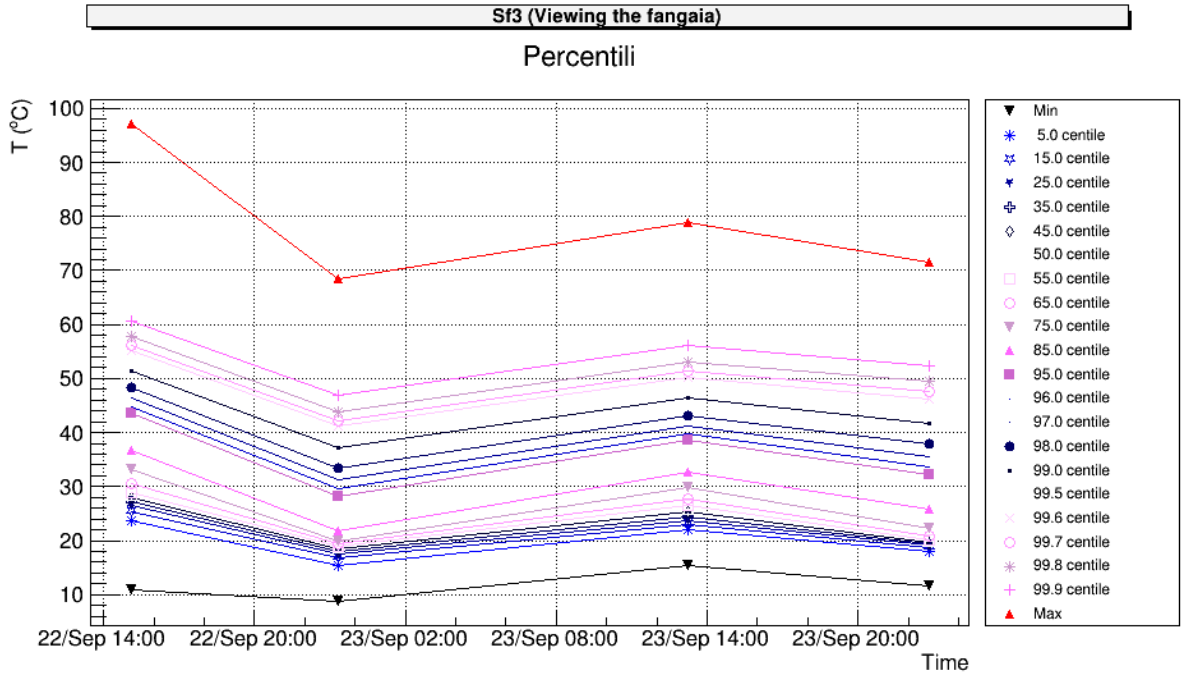

Figure 28. Centiles distribution of the Sf3 panning images.

In the Figure 29, Figure 30 and Figure 31 measurements collected with the Thermotecnix VISIR640 thermal camera are reported for the three sites of Figure 9: soil, “Bocca Nuova” fumarole and “Fangaia”.

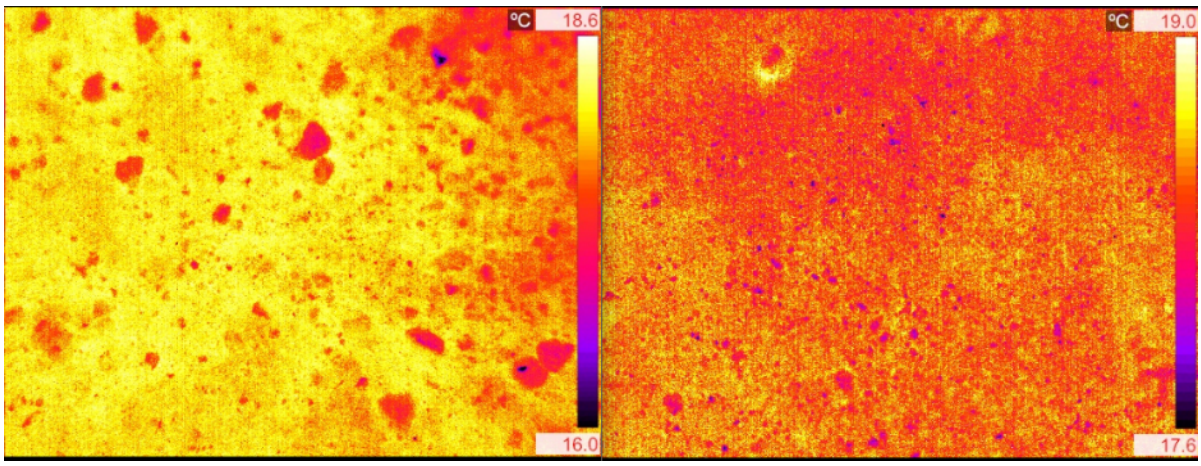

Figure 29. Surface temperature value measured at site A: 22/09/2016 (left), 23/09/2016 (right), both at about 21:00 UTC.

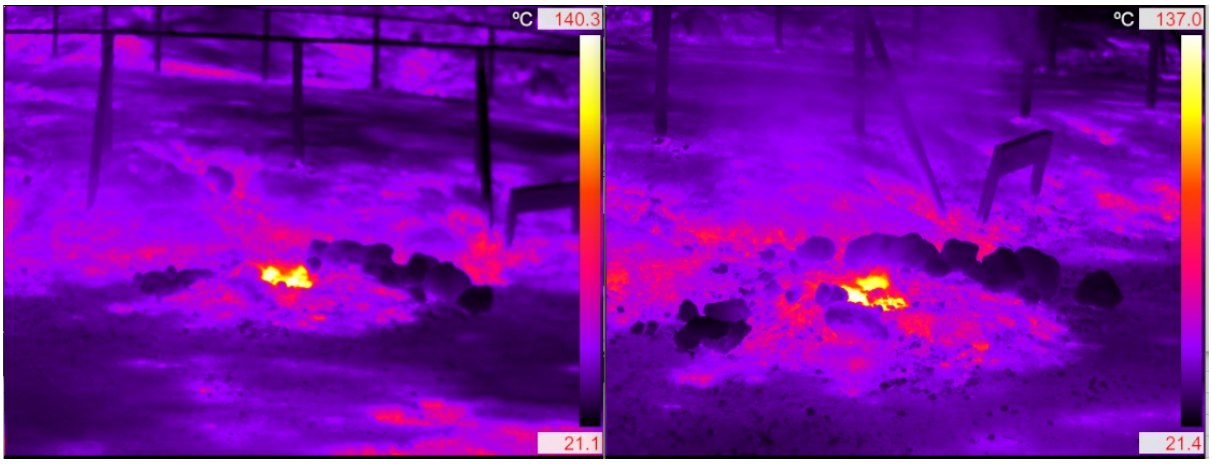

Figure 30. Surface temperature value measured at site B: 22/09/2016 (left), 23/09/2016 (right), both at about 21:00 UTC.

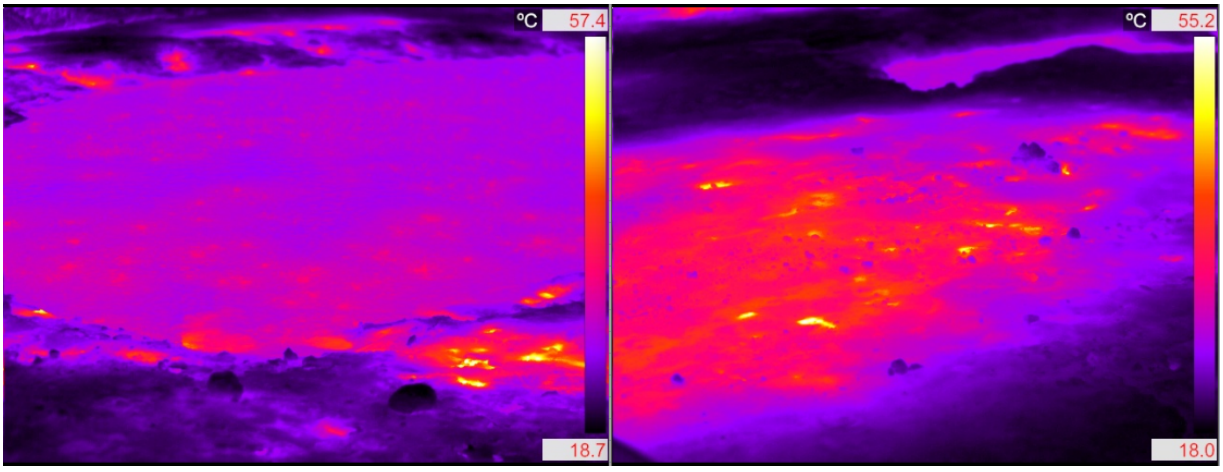

Figure 31. Surface temperature value measured at site C: 22/09/2016 (left), 23/09/2016 (right), both at about 21:00 UTC.

As shown in the figures no thermal variations were detected during the two days. The measurements collected in the sites of Figure 9 are reported in the following table, while a plot with the trend of the temperature measured in both nights is showed in Figure 32.

Latitude	**Longitude**	**Tmax 22/09/2016**	**Tmax 23/09/2016**
40.8273	14.14016	41.9	41
40.8273	14.14016	No measure	36.5
40.82732	14.14006	No measure	49.1
40.82703	14.13938	No measure	44
40.82703	14.13938	57.4	55.2
40.82659	14.16995	27.5	42.5
40.82633	14.13996	20.6	20.3
40.826531	14.14011	22	21.4
40.82629	14.1402	22.2	29.4
40.82629	14.1402	79	74.1
40.82661	14.14038	22.2	21.2
40.82659	14.14047	66.8	73.5
40.82659	14.14047	No measure	55
40.82659	14.14047	No measure	70.4
40.82684	14.14069	51.9	48.9
40.82709	14.14085	90.1	78.8
40.82709	14.14085	79.2	77.3
40.82692	14.14089	45.6	44
40.8269	14.14092	32.1	34.1
40.82689	14.14093	20.9	21.6
40.827204	14.14167	46.5	48.3
40.827204	14.14167	140.3	137
40.827204	14.14167	117.2	122.4
40.82746	14.14149	69.6	38.8
40.82791	14.14156	18.6	19
40.82741	14.14139	20.1	22.9
40.82745	14.14096	91.8	79.7

Table 3. Thermal measurements collected during the two days. The site coordinates are reported.

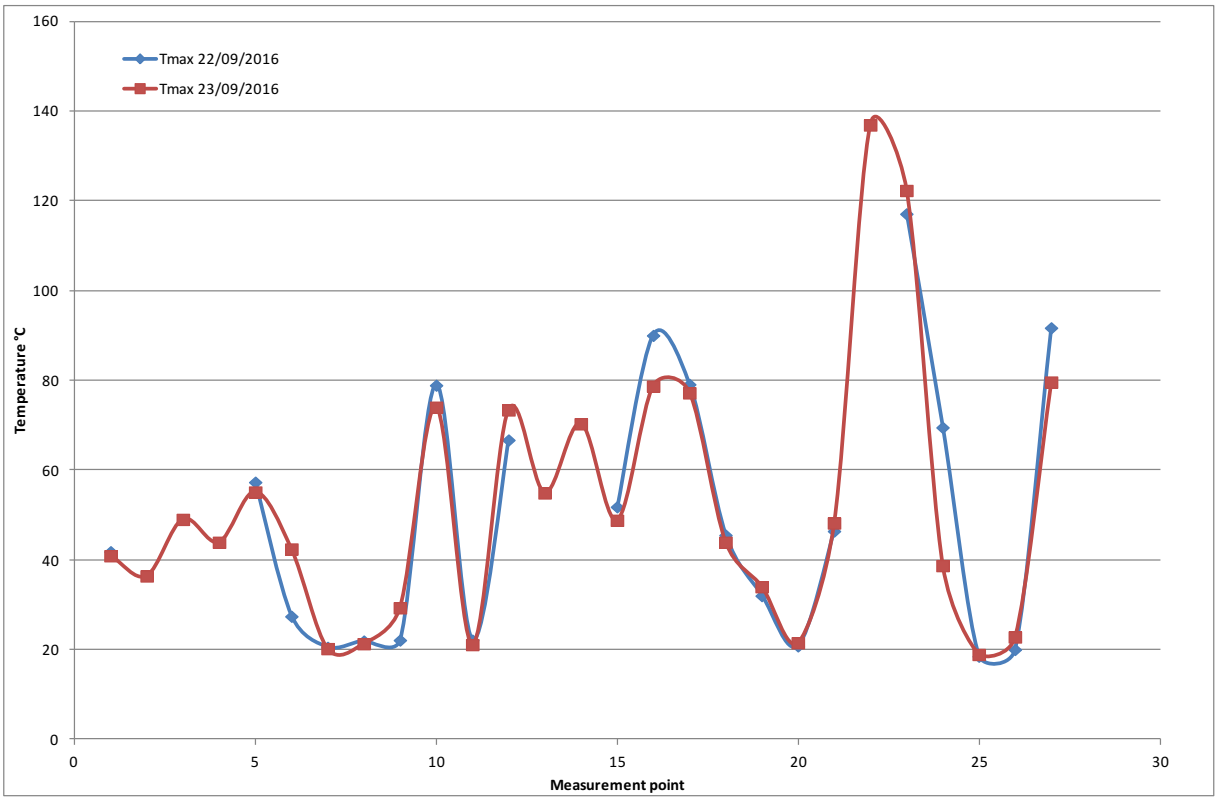

Figure 32. Thermal measurements trend. The hot temperature of about 140° corresponds to the site B ("Bocca Nuova") site of Figure 9.

3.6 ASD FieldSpec

Analysis of surface reflectance data has been proved to be a powerful tool to monitor both alterations in mineralization [Kruse, 2012] and disturbance of the vegetative cycle [Almeida & DeSouza Filho, 2004]. Despite the consensus over the technique, especially exploited for mineral mapping [Sabins, 1999; Van Der Meer et al., 2012; 2014] and hydrocarbon exploration [Van der Meer et al., 2002], very few analyses in the VNIR-SWIR spectral range had been carried out over the Solfatara and the Campi Flegrei hydrothermal system [Sgavetti et al., 2009; Flahaut et al., 2016], especially from in the perspective of monitoring the ongoing volcanic and hydrothermal activity.

Changes in the intensity and/or areal distribution of volcanic and hydrothermal activity could result in subtle changes of surface features, such as altered mineralization or induced stress in vegetation. These evidences could be analyzed and mapped to produce a complementary monitoring tool over the Campi Flegrei volcanic area.

Images obtained by spaceborne instruments have the advantage of a cost-free scheduled acquisition of multi- and hyper-spectral images over the same area, with the trade-off of a reduced spatial and (in the case of multi-spectral imagery) spectral resolution. Limited spatial resolution brings to mixing of spectral signatures from different ground elements falling within the same pixel, whereas limited spectral resolution can prejudice the possibility to discriminate between altered and non-altered materials described by subtle differences in spectral signatures.

The acquisition of field spectra by means of ASD FieldSpec spectrometer, as carried out in this field campaign, has the goal of collecting high-spectral resolution reflectance data from samples of different soils and vegetation in the Solfatara crater, to be used as ground truth in subsequent analyses of space-borne imagery. In particular, our preliminary goal is to establish the variability of spectral signatures within sets of similarly altered (or not altered) materials and between sets of different materials to understand whether or not spectral signatures from altered materials are remarkably different from the ones of an unaltered background. In particular, we intend to explore whether these materials are different enough to support spectral unmixing techniques, supervised land classification methods (such as SAM) or other spectral analyses for specific mineral targets and vegetative indexes.

From this perspective, we started a first campaign to collect spectral data from ground-truth, acquiring reflectance signatures of samples from 25 sites all around the Solfatara crater (Table 2, Figure 10) showing different mineral and vegetative alterations. An optimization process was performed prior to a measurement session and, at each site, a calibration procedure with a Spectralon® panel was carried out. Each site was sampled 30 times in order to determine variances in the measuring procedure. The spectrometer integrated radiation from a FOV of 25°, corresponding to a surface area of about 50 cm^2 at a 1-meter sensor-target distance.

Except in the spectral windows around 1400nm, 1800-1950nm and 2400-2500nm, which are affected by atmospheric effects (absorption, scattering), each set of collected spectra shows a good internal consistency, with standard deviations for reflectance values generally less than 1% in reflectance in the VNIR region and in the 1%-2% range between 1750nm and 2300nm. Higher scattering in recorded reflectance values (St. dev. greater than 5%) is present in the SWIR region above 2350nm.

The few spectral samples collected from the bare soil and altered mineralogy show some possible features useful for spectral characterization of mineralogy, for example comparing spectra from site 15 (Figure 34) to the ones obtained at site 14 (Figure 33) and 16 (Figure 35), it is possible to recognize the effect of the presence of sulfur at the surface by the strong absorption feature below 500 nm. Although in published literature there are examples of mineral mapping (in particular of argillic alterations) by analysis of space borne spectral data, in our case we prefer to collect a wider set of field data before developing an analysis process utilizing satellite data, since the collection of different end-member samples gathered so far is largely incomplete.

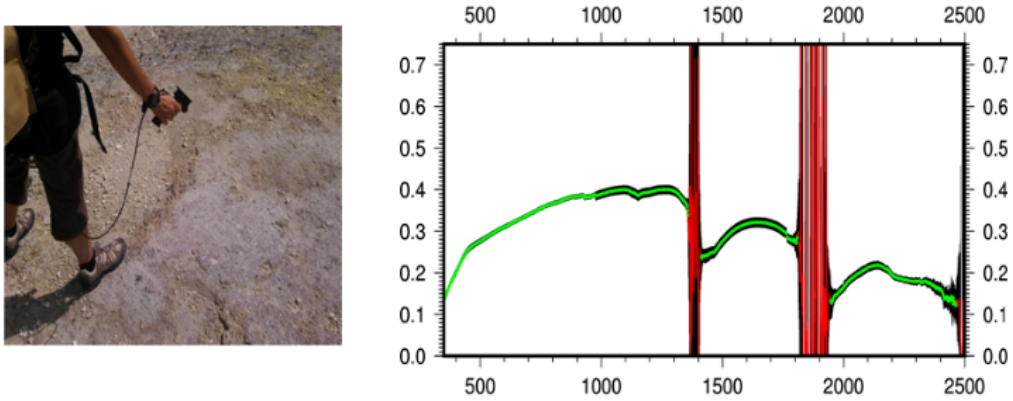

Figure 33. Sampling procedure (left) and reflectance spectrum (right) at site #14, showing argillic alterations. Colored dots represent the mean of reflectance values registered among the set at each wavelength. Dots are depicted in green or red whether the set of reflectance values at the specific wavelength shows a standard deviation below or above 5% (in reflectance values), respectively. Black areas represent the 1-σ confidence levels.

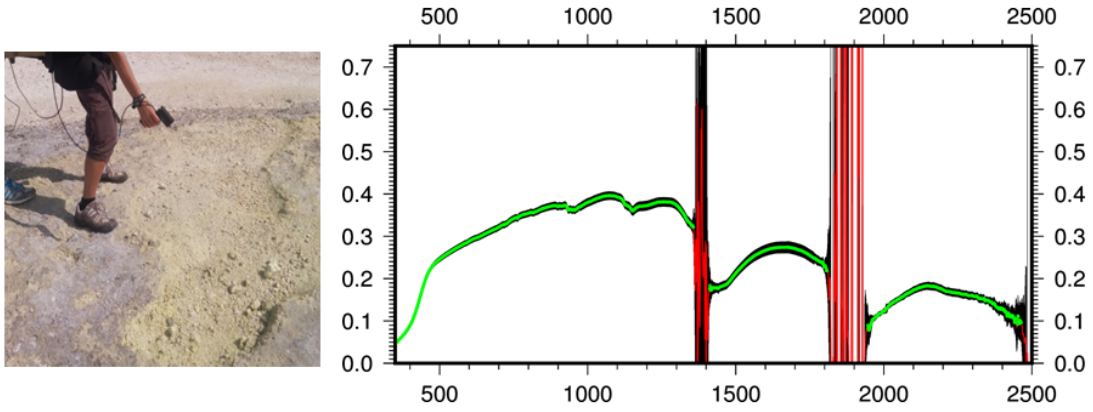

Figure 34. As in Figure 33, for site #15, showing argillic alterations with sulfate hydrates and sulfur.

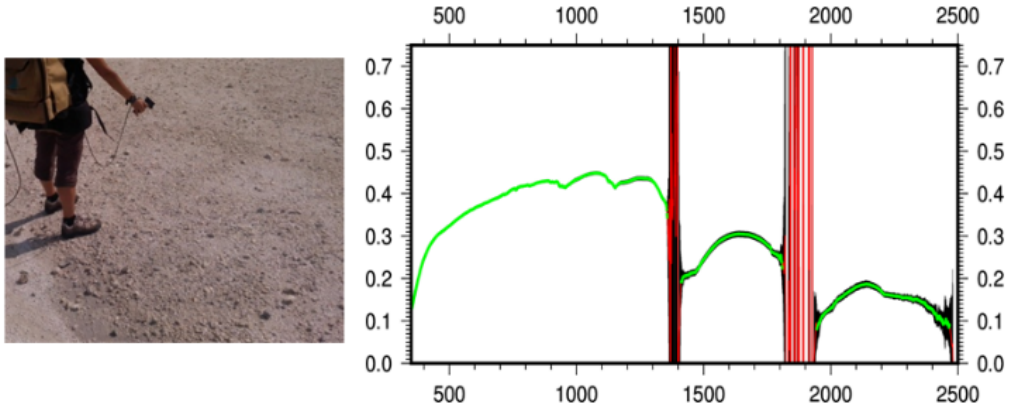

Figure 35. As in Figure 33, for site #16, showing argillic alterations.

Reflectance spectra of vegetation (the examples in figures Figure 36 - Figure 39) show a clear distinction between healthy, chloritic and dry samples that can be mapped by vegetative indexes obtained by mid-resolution space borne sensors. The analysis of VNIR spectra shows differences in signatures from shrubs and grasses, however a first analysis of data suggests that such spectral differences between vegetal land covers might be not pronounced enough to be detectable by sensors with lower spatial/spectral resolution.

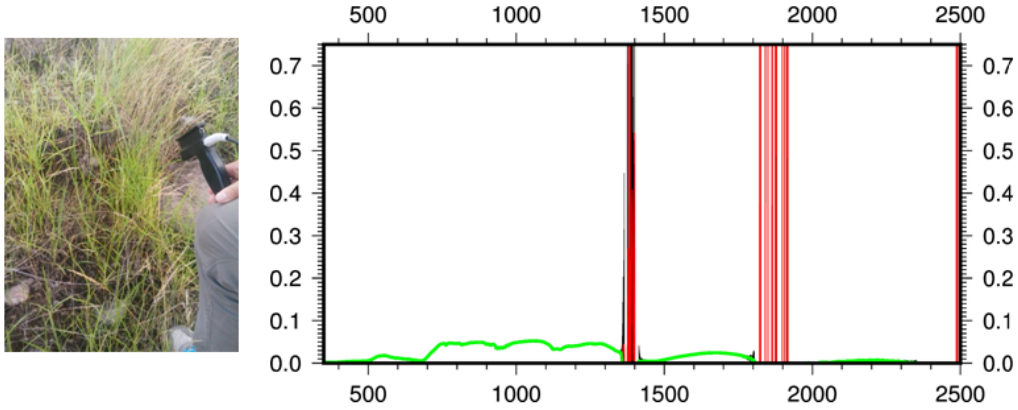

Figure 36. As in Figure 33, for site #10, green healthy grass.

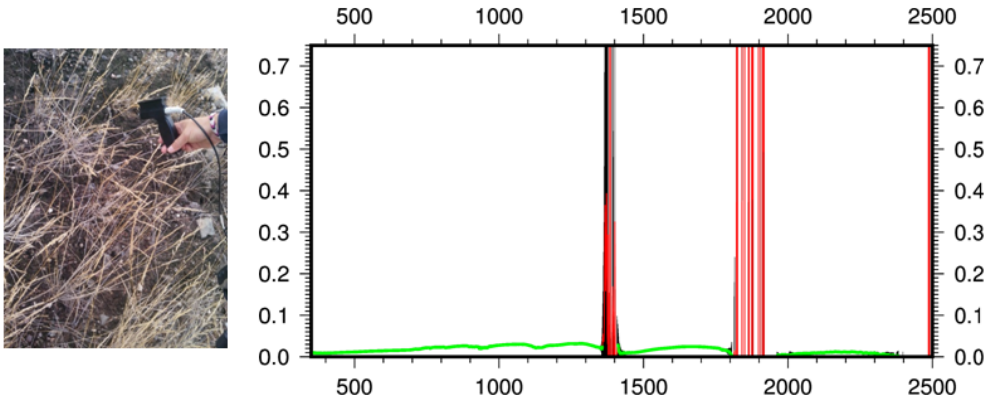

Figure 37. As in Figure 33, for site #11, dried grass.

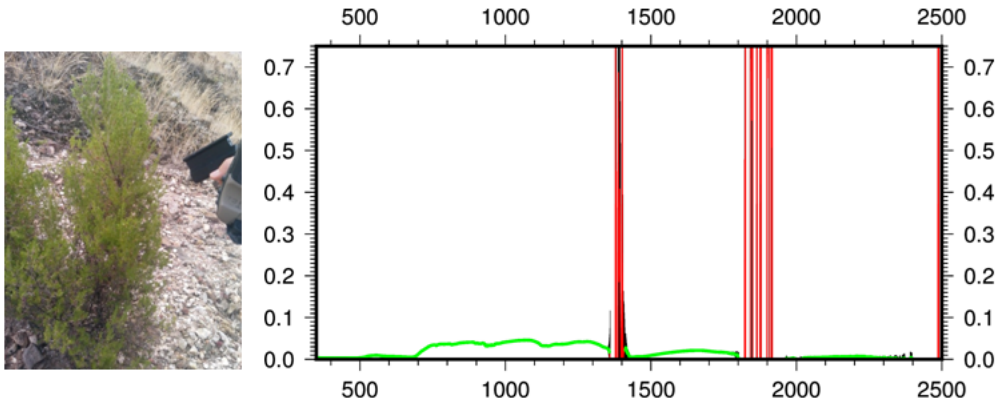

Figure 38. As in Figure 33, for site #12, a green healthy shrub.

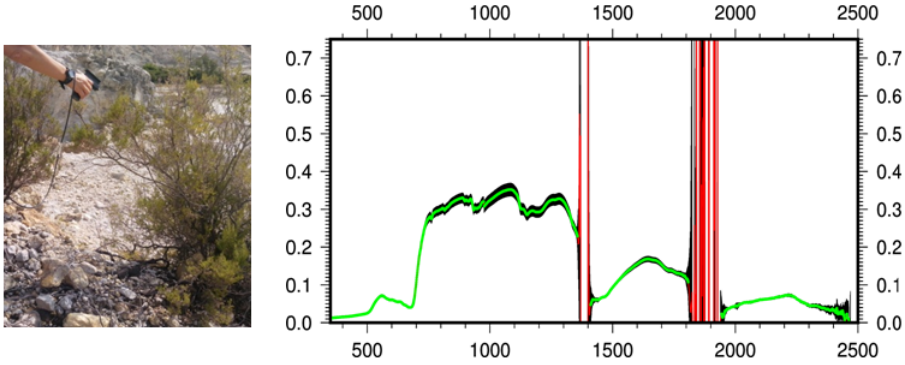

Figure 39. As in Figure 33, for site #25, a partially chloritic shrub.

4. Conclusions

The present work had the goal of describing the testing and improvements of small, economical UAV platforms, with miniaturized instrument payloads, within fumaroles of active Italian volcanoes. With such technology, in situ and proximal remote sensing measurements of volcanic plumes are now possible without risking the lives of scientists and personnel in charge of closely monitoring of volcanic activity. Previous versions of the MiniGAS payload and portable mass spectrometer instrument were already used in the Costa Rica at Turrialba Volcano [Diaz et al., 2010; Pieri et al., 2013], at Solfatara volcano [Silvestri et al., 2015; Diaz et al., 2015; Wright and Diaz, 2015] and at Vulcano Island [Silvestri et al., 2016]. The improvements of these instruments were fully tested by the INGV volcanologists during the 2016 Solfatara campaign, providing important feedback on their operation and indicating their limitations. The systematic collection of in situ data regarding volcanic plume parameters (e.g., temperature, pressure, relative humidity and volcanic gases concentration) offers a valid support to the calibration and validation of remote sensing imagery and to the monitoring of volcanic activity and/or research.

Moreover, the campaign provided a positive result in terms of verifying the instrument portability in areas without easy access. Some considerations can (or will) be done by analyzing the obtained results from the instruments used.

A first partial interpretation of surface reflectance collected data shows that at the FieldSpec hyperspectral scale, it is possible to distinguish between different kinds of vegetation cover (grass, shrub…) and between healthy/stressed vegetation. Downscaling resolutions both spatially and spectrally to meet the characteristics of spaceborne sensors still allows us to monitor the health state of vegetation, but it also makes it infeasible to distinguish between different vegetal species whose spectral signatures are mixed in the same pixel. With respect to mineralization analysis, results obtained so far are not conclusive, even in the favorable case of obtaining hyperspectral, almost point-like, measures provided by the FieldSpec instrument.

The few collected spectra are not exhaustive about the alteration signatures. A new field campaign will be performed on more specific targets related to rock alterations due to hydrothermal and volcanic activity, together with spectral analysis in a controlled environment (laboratory) of selected specimens. A very preliminary observation is that some signatures, such as those given by the presence of sulfur or sulfate hydrates on a background of argillic altered soil (comparing reflectance spectra from sites 14 and 15) could be detected by spaceborne sensors that have bands also in the 400-500nm range.

The Solfatara campaign has been organized taking into account the two scheduled reference satellite acquisitions: Terra ASTER and Landsat 8. Unfortunately, both satellite data were not used due to the presence of clouds on the site. However, considering the spatial and temporal low monthly variability, the Terra ASTER image of September 6 and the Landsat 8 images of September 7, both nighttime acquisitions, were considered in order to compare the results of surface temperature with the fixed cameras.

The land surface temperature measured by satellite is quite comparable with the one acquired by the thermal camera and the discrepancies between observed and modeled temperatures are principally due to several factors such the difference of spatial resolution of satellite data and the "point-size" ground observations.

Finally, this campaign provided a huge volume of data whose interpretation and comparison with different methodologies (collected on site and derived by satellite) is outside of the scope of this report, but that will be more thoroughly analyzed in a follow-on study.

5. Acknowledgements

We want to thank all of our colleagues for their warm hospitality, and the great support provided during the visit of foreign colleagues during the field campaigns at Solfatara volcano. In particular, we thank to Stefano Caliro and enteire staff of the laboratory that allowed Prof. Andres Diaz to assemble and calibrate his equipment. Thanks also to the Administration of the Solfatara Volcano for having allowed us to deploy the instruments in the Naturalistic Park during the day and especially the night.

A special thanks to Thomas Cecere of U.S. Geological Survey for his participation in the field campaign at Solfatara and the English revisions.

Satellite data available from the U.S. Geological Survey.

References

Almeida T.I.R., and De Souza Filho C.R., (2004). *Principal component analysis applied to feature-oriented band ratios of hyperspectral data: a tool for vegetation studies*. International Journal of Remote Sensing, 25(22), 5005-5023.

ASD, (2002). *Fieldspec FR User's Guide*. Analytical Spectral Devices Inc., Boulder, CO, 136pp.

Badalamenti B., Liotta M., Valenza M., (2001). *An automatic system for continuous monitoring of CO sub 2, H sub 2 S, SO sub 2 and meteorological parameters in the atmosphere of volcanic areas,* Geochem. Trans., 2, 1–5, doi:10.1186/1467-4866-2-30.

Barsi J.A., Barker J.L., Schott J.R., (2003). *An Atmospheric Correction Parameter Calculator for a Single Thermal Band Earth-Sensing Instrument*. IGARSS03, 21-25 July 2003, Centre de Congres Pierre Baudis, Toulouse, France.

Chiodini G., Frondini F., Cardellini C., Granieri D., Marini L., Ventura G., (2001). *CO_2 degassing and energy release at Solfatara volcano, Campi Flegrei, Italy.* Journal of Geophysical Research: Solid Earth, Volume 106, Issue B8, pp. 16, 213-16, 221.

Chiodini, G., Vilardo G., Augusti V., Granieri D., Caliro S., Minopoli C., and Terranova C., (2007). *Thermal monitoring of hydrothermal activity by permanent infrared automatic stations: Results obtained at Solfatara di Pozzuoli, Campi Flegrei (Italy)*. J. Geophys. Res., 112, B12206, doi:10.1029/2007JB005140.

Diaz J.A, Pieri D., Arkin R., Gore E., Griffin T.P., Fladeland M., Bland G., Soto C., Madrigal Y., Castillo D., Rojas E., Achi S., (2010). *Utilization of in situ airborne MS-based instrumentation for the study of gaseous emissions at active volcanoes.* International Journal of Mass Spectrometry, 295, 105 – 112. doi:10.1016/j.ijms.2010.04.013

Diaz J.A., Pieri D., Wright K., Sorensen P., Kline-Shoder R., Arkin CR., Fladeland M., Bland G., Buongiorno M.F., Ramirez C., Corrales E., Alan A., Alegria O., Diaz D. and Linick J., (2015). *Unmanned aerial mass spectrometer systems for in-situ volcanic plume analysis.* J. Am. Soc. Mass. Spectrom. 26(2): 292-304. doi: 10.1007/s13361-014-1058-x. Epub 2015 Jan 15.

Flahaut J., Bishop J.L., Daniel I., Silvestro S., Tedesco D., and Quantin C., (2016). *Spectral characterization of the sulfate deposits at the Mars analog site of La Solfatara (Italy)*. 47th Lunar and Planetary Science Conference, abstract #2233.

Gillespie A., Rokugawa S., Matsunaga T., Cothern J.S., Hook S.J. and Kahle A.B., (1998). *A temperature and emissivity separation algorithm for Advanced Spaceborne Thermal Emission and Reflection Radiometer (ASTER) images*. IEEE Transactions on Geoscience and Remote Sensing, 36(4): 1113-1126.

Kruse F.A., (2012). *Mapping surface mineralogy using imaging spectrometry*, Geomorphology, 137(1), 41-56.

Musacchio M., Amici S., Silvestri M., Teggi S., Buongiorno M.F., Silenzi S., Devoti S., (2007). *Application of CIRILLO: a new atmospheric correction tool on Castel Porziano Beach (CPB)*. Proc. SPIE 6749, Remote Sensing for Environmental Monitoring, GIS Applications, and Geology VII, 674935, doi:10.1117/12.752670.

Pieri D., Diaz J. A., Bland G., Fladeland M., Madrigal Y., Corrales E., Alegria O., Alan A., Realmuto V., Miles T. and Abtahi A., (2013). *In situ observations and sampling of volcanic emissions with NASA and UCR unmanned aircraft, including a case study at Turrialba Volcano, Costa Rica*. The Geological Society of London 2013, Geological Society, London, Special Publications, 380, 321–352. http://dx.doi.org/10.1144/SP380.13

Roberts T.J., Braban C.F., Oppenheimer C., Martin R.S., Freshwater R.A., Dawson D.H., Griffiths P.T., Cox R.A., Saffell J.R., Jones R.L. (2012), *Electrochemical sensing of volcanic gases,* Chem. Geol., 332–333 (2012), pp. 74-91.

Roberts T.J., Saffell J.R., Oppenheimer C., Lurton T., (2014). *Electrochemical sensors applied to pollution monitoring: Measurement error and gas ratio bias — A volcano plume case study.* Journal of Volcanology and Geothermal Research, Volume 281, 15 June 2014, Pages 85-96 https://doi.org/10.1016/j.jvolgeores.2014.02.023

Sabins F.F., (1999). *Remote sensing for mineral exploration*. Ore Geology Reviews, 14, 157-183.

Sansivero, F., Scarpato G., and Vilardo G., (2013). *The automated infrared thermal imaging system for the continuous long-term monitoring of the surface temperature of the Vesuvius crater*. Ann. Geophys., 56, S0454, doi:10.4401/ag-6460

Sgavetti M., Pompilio L., Roveri M., Manzi V., Valentino G.M., Lugli S., Carli C., Amici S., Marchese F., and Lacava T., (2009). *Two geologic systems providing terrestrial analogues for the exploration of sulfate deposits on Mars: Initial spectral characterization*. Planetary and Space Science, 57(5-6), 614-627.

Silvestri M., Diaz J.A., Marotta E., Musacchio M., Buongiorno M.F., Sansivero F., Cardellini C., Pieri D., Amici S., Bagnato E., Beddini G., Belviso P., Carandente A., Colini L., Doumaz F., Peluso R., Spinetti C., (2015). *Use of multiple in situ and remote sensing instruments and techniques at Solfatara field campaign for measurements of CO_2, H_2S and SO_2 emissions: special demonstration on unmanned aerial systems*. Quaderni di Geofisica, n.129, http://www.ingv.it/editoria/quaderni/2015/quaderno129/

Silvestri M., Diaz J.A., Vita F., Musacchio M., Puchalla J., Falcone S., Buongiorno M.F., Doumaz F., Wright K., (2016). *Improved instruments for volcanic plume observation for monitoring purpose: Solfatara and Vulcano island preliminary result*. Rapporti Tecnici INGV, ISSN 2039-7941, Anno 2016, N. 349, 1- 44, http://www.ingv.it/editoria/rapporti/2016/rapporto349/

Van der Meer F., van Dijk P., van der Werff H., and Yang H., (2002). *Remote sensing and petroleum seepage: a review and case study*. Terra Nova, 14. 1-17.

Van der Meer F.D., Van der Werff H.M.A., Van Ruitenbeek F.J.A., Hecker C.A., Bakker W.H., Noomen M.F., van der Meijde M., Carranza E.J.M., de Smeth J.B., Woldai T., (2012). *Multi- and hyperspectral geologic remote sensing: a review*. Int. J. Appl. Earth Observ. Geoinform., 14 (1), pp. 112–128.

Van der Meer F., Hecker C., van Ruitenbeek F., van der Werff H., de Wijkerslooth C., and Wechsler C., (2014). *Geologic remote sensing for geothermal exploration: A review*. International Journal of Applied Earth Observation and Geoinformation, 33. 255-269.

Vilardo, G., Sansivero F., and Chiodini G., (2015). *Long-term TIR imagery processing for spatiotemporal monitoring of surface thermal features in volcanic environment: A case study in the Campi Flegrei (Southern Italy)*. J. Geophys. Res. Solid Earth, 120, 812–826, doi:10.1002/2014JB011497

Wright K. and Diaz J.A., (2015). *In-situ Volcanic Plume Monitoring at Solfatara Volcano and Vulcano Island, Italy with Small Portable Mass Spectrometer Systems designed for Field Deployment and Unmanned Aerial Vehicles (UAV).* 10th Workshop on Harsh-Environment Mass Spectrometry September 13–16, 2015, Baltimore.

WebSite

https://asterweb.jpl.nasa.gov/
www.exelisvis.com
https://landsat.usgs.gov/landsat-8

ISSN 1590-2595

Quaderni di Geofisica

http://istituto.ingv.it/l-ingv/produzione-scientifica/quaderni-di-geofisica/

I Quaderni di Geofisica coprono tutti i campi disciplinari sviluppati all'interno dell'INGV, dando particolare risalto alla pubblicazione di dati, misure, osservazioni e loro elaborazioni anche preliminari, che per tipologia e dettaglio necessitano di una rapida diffusione nella comunità scientifica nazionale ed internazionale. La pubblicazione on-line fornisce accesso immediato a tutti i possibili utenti. L'Editorial Board multidisciplinare garantisce i requisiti di qualità per la pubblicazione dei contributi.

ISSN 2039-7941

rapporti tecnici INGV

http://istituto.ingv.it/l-ingv/produzione-scientifica/rapporti-tecnici-ingv/

I Rapporti Tecnici INGV pubblicano contributi, sia in italiano che in inglese, di tipo tecnologico e di rilevante interesse tecnico-scientifico per gli ambiti disciplinari propri dell'INGV. La collana Rapporti Tecnici INGV pubblica esclusivamente on-line per garantire agli autori rapidità di diffusione e agli utenti accesso immediato ai dati pubblicati. L'Editorial Board multidisciplinare garantisce i requisiti di qualità per la pubblicazione dei contributi.

ISSN 2039-6651

Miscellanea INGV

http://istituto.ingv.it/l-ingv/produzione-scientifica/miscellanea-ingv/

La collana Miscellanea INGV nasce con l'intento di favorire la pubblicazione di contributi scientifici riguardanti le attività svolte dall'INGV (sismologia, vulcanologia, geologia, geomagnetismo, geochimica, aeronomia e innovazione tecnologica). In particolare, la collana Miscellanea INGV raccoglie reports di progetti scientifici, proceedings di convegni, manuali, monografie di rilevante interesse, raccolte di articoli ecc..

Coordinamento editoriale e impaginazione
Centro Editoriale Nazionale | INGV

Progetto grafico e redazionale
Daniela Riposati | Laboratorio Grafica e Immagini | INGV

Via di Vigna Murata, 605
00143 Roma
Tel. +39 06518601 Fax +39 065041181

http://www.ingv.it

Istituto Nazionale di Geofisica e Vulcanologia